Analysis of the characterisitic perturbations spectrum of the exact invariant solution of the microconvection equations

V.B. Bekezhanova[a,b]

[a]*Institute of Computational Modeling SB RAS, Akademgorodok 50/44, Krasnoyarsk, 660036, Russia*
[b]*Siberian Federal University, Svobodny pr. 79, Krasnoyarsk, 660041, Russia*

Abstract

The properties of an exact invariant solution of the equations of microconvection of isothermally incompressible liquids have been investigated. The solution describes a stationary fluid flow in a vertical channel. The temperature or heat flux can be given at the solid boundaries of the channel. A classification of the solutions and their physical interpretation are suggested. In accordance with the classification the solutions describe different types of flows. The solution of the stability problem of all classes of flows in the vertical channel with the given temperature on the walls is presented. The structure of the spectrum of small non-stationary spatial perturbations for the model medium (silicon dioxide melt) has been studied, depending on the configuration of the perturbation wave, thickness channel, thermal and gravitational effects. The formation regularities of different types of the thermal and hydrodynamic disturbances have been determined. The interaction of the thermal and hydrodynamic perturbations leads to the formation of various convective structures. Typical patterns of the velocity and temperature perturbations and relations of critical characteristics of the instability are presented, depending on the problem parameters. The most dangerous mechanisms change from hydrodynamic to thermal ones with the variation of the viscous and thermal liquid properties.

Key words: microconvection, exact solution, stability

Email address: vbek@icm.krasn.ru (V.B. Bekezhanova)

PACS: 04.25.dc, 05.60.-k, 02.70.-c

1. Introduction

Microconvective phenomena in different systems have been the subject of the detailed investigation in the last few decades (for a review, see [1, 2, 3, 4, 5]). The traditional areas of the application of nonisothermal microconvective flows are chemical engineering, materials science, thermophysics. Fluid technologies are applied in the growth of ultra-pure crystals, in microchips for biological systems, in micropumps and micro heat exchangers in power systems and in life-support setups of orbital platforms.

Fluid motion under the joint action of mass, surface forces and thermal loads is the subject of extensive theoretical and experimental investigations. The study of the convective processes is complicated by nonstationarity and nonlinearity. Often, there are some difficulties in the experiments. The first of them is the reconstruction of the conditions in which the investigated phenomenon is observed. Other difficulties are connected with highly accurate measurements of the characteristics and great resource consumption.

Obtaining crystals with high uniformity and structure perfection is a complex technological problem, which stimulates theoretical and experimental investigations. It results in the intensive development of space materials science. The aim of the comprehensive study of the processes responsible for the formation of macro and micro inhomogeneities in crystals is to analyze the influence of the dissimilar physical and chemical factors on the convective processes in melts and solutions, which are used for ultra-pure high-quality crystals [3, 6]. It is known that under the terrestrial conditions the gravity forces impede obtaining materials which are uniform in the distribution of components and phases. Thermogravitational convection results in the instability of the crystal growth parameters. In a zero-g field greater advantageous conditions arise for obtaining a homogeneous monocrystal without structural defects. But in space experiments it is specified that in prolonged weightlessness there occur peculiar hydrodynamical processes resulting in arising macro and micro inhomogeneities. Physical reasons for these processes are connected with the action of small forces of gravitational and inertial nature (for a review, see [7, 8]).

It is known that the arising cellular perturbations worsen the quality and properties of the obtained pattern [6, 9, 10, 11, 12, 13, 14]. Hence, the

efficiency of the methods of growing ultra-pure crystals from liquid melts can be enhanced by stabilizing the convective flows of the working fluid. Therefore, special emphasis is placed on the study of the factors causing the formation of spatial defects in crystals. Knowing the critical mechanisms enables one to control the technological process through external effects and facilitates the elaboration of methods of obtaining high quality patterns with the pre-assigned structure and properties both under zero gravity and in the mass forces field.

Investigations in microgravity resulted in the necessity of revising the fundamental constructs of the Oberbeck – Boussinesq model and, as a consequence, in the construction of new exact solutions and study of new problems on the stability of convective flows. As a result of elaborating the Navier – Stokes equations in the Boussinesq approximation, the microconvection equations were obtained by Puknachev V.V. [15, 16, 17]. The new model allows one to extend the applicability boundaries of the classical models. Within a few years similar equations were suggested by Perera P.S. and Sekerka R.F. for the investigation of the concentration convection [18]. Mathematical models on the basis of the Navier-Stokes equations were described in [19]. In the framework of the models the convection, heat and mass exchange results were obtained for technical, technological and geophysical applications. Nonstandard treatments for investigating nonlinear hydrodynamics equations, the construction of the exact solution classes of different convection models were described in [20]. In [3, 21] the investigation results for gravitational and nongravitational convection under different micro accelerations, including the limit case of theoretical weightlessness were generalized and spatial convective flows realized in the space flight were studied. The mathematical models of convection in weak force fields and on the microscales and analytical investigations of liquid motions performed on the basis of the models were presented in [22, 23]. Due to the known analogy between the transfer processes on the microscales and in microgravity [22] the results of the convection study can be highly useful in view of miniaturization of different types of electronic devices.

Dissimilar outer and internal factors affect the character of convective flows in different systems. The intensity of the liquid motion can rise and it can become unstable as a result of the interaction of these factors. As compared with isothermal flows the convective ones have a wide spectrum of disturbances and are characterized by various mechanisms leading to instability. The stable state of equilibrium or motion of the working fluid is the

primary condition of the correct functioning of the experimental or industrial equipment using fluidic systems. Therefore, the need for modeling convective flows is dictated by the intention to exactly forecast the behavior of the liquid and to prevent possible crisis phenomena. Thus, in the process of crystal growth various structural defects of the obtained patterns correspond to different types of perturbations. The convective heat and mass exchange causes longitudinal and transverse macro inhomogeneities. The temperature oscillations associated with convective instability in melts induce micro nonuniformities (streaked structure).

Recently, special attention has been paid to the construction and investigation of exact solutions describing the convective flows [20, 24]. The exact solutions allow one to investigate in detail the influence of various physical factors on the character of flows, to accurately predict the results of the laboratory experiments and to perform the analysis and find the conditions to ensure the stability.

This is particularly valuable to an exact solution to have a group nature, since precisely a group origination of a solution ensures its physical plausibility and realizability. The microconvection model is based on the exact mass and momentum conservation laws [17, 22]. Thus, the basic equations have been formulated on the basis of postulates, which imply the natural symmetry properties of space – time and of a fluid moving in the space. Therefore, the exact solution, that has the group nature, conserves the symmetry properties provided by the derivation of the governing equations. It is not surprising that the microconvection equations possess the group properties and admit a large group of transformations [20]. The main transformation group of the system was calculated in [25] for $\boldsymbol{g} = (0, -g, 0)$, $g = \text{const}$, $\boldsymbol{g}$ is the gravitational vector. On this basis, a number of exact solutions of microconvection equations was constructed [26, 27, 28, 29]. An optimal system of the first and second-order subalgebras were calculated by Rodionov A.A. in [27] and [22], respectively. Using the operators of the optimal systems of the first and second-order subalgebras several examples of factor-systems in invariant variables were constructed [27].

Up to the present only one exact solution has been interpreted and studied in stationary [26] and non-stationary [22, 29] cases. The solution was applied only for simple geometry, such as a vertical channel. For other geometries exact solutions have not been studied yet. Only numerical modeling of convection was performed in the framework of the microconvection model in the non-stationary case for the following geometries: a long rectangle, a ring

domain with solid boundaries, a semicircle with a free boundary and ring domain with a free boundary [29, 30]. Comparison of convection regimes and its thermal and hydrodynamic characteristics calculated on the basis of the Oberbeck – Boussinesq and microconvection models was performed in [30, 31] by numerical modeling. Both qualitative and quantitative differences for temperature and velocity fields and for trajectories of liquid particles were found.

Some results, concerning the stability of the above mentioned exact solution in the stationary case, have been obtained [32, 33]. In [32] the plane perturbations of the exact solution were considered and comparison with results, obtained for analogical problem in the framework of the Oberbeck – Boussinesq model, was performed. Upon that, the Dirichlet boundary conditions were imposed for the temperature function on the rigid walls. In [33] the structure of spatial disturbances of the exact solution was studied in the framework of the Neumann problem. Stability of equilibrium in a plane horizontal channel with solid walls and with a free boundary has been studied in [34] and [35]. Comparison of the critical characteristics of the linear stability of some flows and equilibrium configurations obtained in the framework of microconvection and the Oberbeck – Boussinesq models is presented in [36]. Decrease of the threshold characteristics of stability was revealed for the microconvection model.

In the present work the exact invariant solution of the microconvection equations describing the convective flow in the vertical channel at a given temperature on the channel walls is investigated. The properties of spatial characteristic perturbations of the basic flow and the influence of the problem parameters on their structure and mechanisms leading to the change in the flow pattern are investigated in the frame of the linear theory. The results would allow one to solve the problems of convection suppression in melts in view of the improvement of the crystal microuniformity and to define the possibilities to control the convective processes by changing the geometry of the volume filled with the melts, way of heat supply and gravitational effect.

2. General equations and governing parameters

For the description of the convective flows the microconvection equations of the isothermally incompressible liquid are used

$$\operatorname{div} \boldsymbol{w} = 0, \tag{2.1}$$

$$\boldsymbol{w}_t + \boldsymbol{w}\cdot\bigtriangledown\boldsymbol{w} + \beta\chi(\bigtriangledown\theta\cdot\bigtriangledown\boldsymbol{w} - \bigtriangledown\boldsymbol{w}\cdot\bigtriangledown\theta) + \beta^2\chi^2(\triangle\theta\bigtriangledown\theta -$$
$$-\bigtriangledown|\bigtriangledown\theta|^2/2) = (1+\beta\theta)(-\bigtriangledown q + \nu\triangle\boldsymbol{w}) + \boldsymbol{g}, \tag{2.2}$$
$$\theta_t + \boldsymbol{w}\cdot\bigtriangledown\theta + \beta\chi|\bigtriangledown\theta|^2 = (1+\beta\theta)\chi\triangle\theta. \tag{2.3}$$

Here $\boldsymbol{w}$ is the modified velocity vector, q is the modified pressure, θ is the temperature, β, χ, ν are the constant coefficients of thermal expansion, heat diffusivity and kinematic viscosity, respectively. The modified velocity $\boldsymbol{w}$ and pressure q are related to the corresponding true (physical) characteristics and have the form

$$\boldsymbol{w} = \boldsymbol{v} - \beta\chi\bigtriangledown\theta, \quad q = \rho_0^{-1}(p - \lambda\,\mathrm{div}\boldsymbol{v}) - \beta(\nu-\chi)\chi\triangle\theta,$$

where $\boldsymbol{v} = (v_1, v_2, v_3)$ is the true velocity vector, p is the true pressure, ρ_0 is the typical density value, λ is the coefficient of the second viscosity.

Note 1. System (2.1)–(2.3) for new unknown functions $\boldsymbol{w}$, q, θ was obtained from the exact equations of continuity, momentum and energy in [17]. Here, the fluid density depends on temperature $\rho = \rho_0(1+\beta\theta)^{-1}$ and does not depend on pressure.

Note 2. Momentum equation (2.2) can be written in another form. Actually, we have $\bigtriangledown\theta\cdot\bigtriangledown\boldsymbol{w} - \bigtriangledown\boldsymbol{w}\cdot\bigtriangledown\theta = \bigtriangledown\theta\cdot\bigtriangledown\boldsymbol{w} - \bigtriangledown\theta\cdot(\bigtriangledown w)^* = \mathrm{rot}\,\boldsymbol{w}\times\bigtriangledown\theta$. Also, $\bigtriangledown|\bigtriangledown\theta|^2/2 = \bigtriangledown\theta\cdot\bigtriangledown(\bigtriangledown\theta)$, then $\triangle\theta\bigtriangledown\theta - \bigtriangledown|\bigtriangledown\theta|^2/2 = [\mathrm{div}(\bigtriangledown\theta)I -$ $-\partial(\bigtriangledown\theta)/\partial(\boldsymbol{x})]\bigtriangledown\theta = \mathrm{div}[\bigtriangledown\theta\otimes\bigtriangledown\theta - |\bigtriangledown\theta|^2 I]$, where I is the unit tensor, $\otimes$ denotes the tensor product. Taking into account the last Formulae, equation (2.2) is rewritten in the form

$$\boldsymbol{w}_t + \boldsymbol{w}\cdot\bigtriangledown\boldsymbol{w} + \beta\chi\mathrm{rot}\boldsymbol{w}\times\bigtriangledown\theta + \beta^2\chi^2\mathrm{div}[\bigtriangledown\theta\otimes\bigtriangledown\theta - |\bigtriangledown\theta|^2 I] =$$
$$= (1+\beta\theta)(-\bigtriangledown q + \nu\triangle\boldsymbol{w}) + \boldsymbol{g}. \tag{2.2}'$$

Let $\boldsymbol{x} = (x, y, z)$, a is the linear scale, θ_* is the typical temperature drop. Nondimensional variables and functions are introduced by the following relations

$$\boldsymbol{\zeta} = (\zeta, \xi, \vartheta) = \frac{\boldsymbol{x}}{a}, \quad \tau = \frac{\chi}{a^2}t, \quad \boldsymbol{w}' = \frac{a}{\chi}\boldsymbol{w}, \quad \theta' = \frac{\theta}{\theta_*}, \quad q' = \frac{a^2}{\nu\chi}q. \tag{2.4}$$

Then, equations (2.1), (2.2)′, (2.3) are rewritten in the nondimensional form (primes are omitted):

$$\boldsymbol{w}_\tau + \boldsymbol{w}\nabla\boldsymbol{w} + \varepsilon\ \mathrm{rot}\boldsymbol{w}\times\nabla\theta + \varepsilon^2\mathrm{div}(\nabla\theta\otimes\nabla\theta - |\nabla\theta|^2 I) =$$

$$= (1+\varepsilon\theta)(-\nabla\bar{q}+\Delta\boldsymbol{w})\mathrm{Pr}-\varepsilon\boldsymbol{\eta}(\tau)\mathrm{Pr}\,\theta, \tag{2.5}$$

$$\operatorname{div}\boldsymbol{w}=0, \tag{2.6}$$

$$\theta_\tau+\boldsymbol{w}\cdot\nabla\theta+\varepsilon|\nabla\theta|^2=(1+\varepsilon\theta)\Delta\theta, \tag{2.7}$$

where $\bar{q}=q-a^3\boldsymbol{g}(t)\cdot\boldsymbol{\zeta}/\nu\chi$ is the analog of the modified pressure, $\varepsilon=\beta\theta_*$ is the Boussinesq parameter, $\mathrm{Pr}=\nu/\chi$ is the Prandtl number, $\boldsymbol{\eta}=a^3\boldsymbol{g}(t)/\nu\chi$ is the vector parameter of microconvection, which is a new similarity criterion. The last term in the right side of (2.5) contains the multiplier $\varepsilon\boldsymbol{\eta}(\tau)\mathrm{Pr}$, which defines the vector of the Grashof numbers $\mathbf{Gr}=\varepsilon\boldsymbol{\eta}(\tau)\mathrm{Pr}=$ $=\beta\theta_*a^3\boldsymbol{g}(t)/\chi^2$. If $g=|\boldsymbol{g}|$, then, we have the usual Grashof number $\mathrm{Gr}=\beta\theta_*ga^3/\chi^2$ which is one of the basic parameters as with ε and Pr in the theory of thermal gravitational convection.

Note 3. Compare the contribution of the buoyancy force and effect of the volumetric expansion on the formation of the velocity field to have some qualitative information. The order of the velocity of the flow induced by the buoyancy force is $\beta\theta_*a^2\nu^{-1}|\boldsymbol{g}|$ for the moderate Grashof number. The contribution of the volumetric expansion to the velocity field is evaluated by $\beta\theta_*a^{-1}\chi$. Thus, the parameter $\eta=|\boldsymbol{g}|a^3/\nu\chi$ has simple physical meaning and is equal to the ratio of orders of the velocities generated by the volumetric expansion and buoyancy factor. The Oberbeck – Boussinesq approximation is inapplicable to describe convection, if $\eta\le 1$ [17]. The smallness of η can be ensured due to the smallness of the gravity acceleration (convection in microgravity), length scale (convection on the microscale) or due to the large product of the viscosity and thermal diffusivity coefficients. In all the above mentioned cases the term "microconvection" is used. Let us introduce the notations $g_0=9.8\ \mathrm{m/s^2}$.

The microconvection model is characterized by the non-solenoidality of the true (physical) velocity field $\boldsymbol{v}$. If we suppose that the specific volume linearly depends on the temperature then the original system of the microconvection equations can be written for new unknown functions $\boldsymbol{w}$, q and θ. In [22] it was shown, that the dependence of density on temperature $\rho=\rho_0(1+\beta\theta)^{-1}$ is unique one that enables to introduce the solenoidal modified velocity. It should be noted that this dependence is physically plausible (the decrease of density takes place with increasing temperature for most liquids). At small values of the Boussinesq number ε it is equivalent to the classical dependence within the accuracy of ε^2. Solenoidality property of the modified velocity $\boldsymbol{w}$ allows one to obtain all necessary results about the

solvability of the boundary value problems and to introduce an analogue of the stream function for plane problems. It should be emphasized, that the true velocity vector $\boldsymbol{v}$ is not the solenoidal one. Consideration of non-solenoidality of the velocity field leads to appearance of the non-Boussinesq effects in fluid flows, which are not confirmed with the help of the classical convection theory.

Let an isothermally incompressible liquid fill the domain Ω with the boundary Σ. The following conditions for the velocity and temperature are imposed on Σ:

$$\boldsymbol{w} + \beta\chi \bigtriangledown \theta = 0, \qquad \theta = \theta_w(\boldsymbol{x}, t), \qquad \boldsymbol{x} \in \Sigma\,, \tag{2.8}$$

or

$$\boldsymbol{w} + \beta\chi \bigtriangledown \theta = 0, \quad k\,\frac{\partial\theta}{\partial n} = d(\boldsymbol{x}, t), \qquad \boldsymbol{x} \in \Sigma\,. \tag{2.9}$$

Here, θ_w, d are the given temperature and heat flux, respectively, k is the thermal conductivity coefficient. In the non-dimensional variables the no-slip condition has the form $\boldsymbol{w} + \varepsilon\nabla\theta = 0$, then (2.8) and (2.9) can be written as

$$\boldsymbol{w} + \varepsilon\nabla\theta = 0, \qquad \theta = \theta_w(\boldsymbol{\zeta}, \tau), \qquad \boldsymbol{\zeta} \in \Sigma\,, \tag{2.10}$$

$$\boldsymbol{w} + \varepsilon\nabla\theta = 0, \qquad \partial\theta/\partial n = D(\boldsymbol{\zeta}, \tau), \qquad \boldsymbol{\zeta} \in \Sigma\,, \tag{2.11}$$

where D is the non-dimensional heat flux.

If the modified velocity $\boldsymbol{w}$ is equal to some function on a boundary, then this function characterizes the value of the temperature gradient on the boundary (trace of the temperature gradient). This fact results in the necessary condition of solvability of the problem; the condition is the equality of the integral heat flux to zero on the boundary. Taking into account the relation between $\boldsymbol{w}$ and $\boldsymbol{v}$, the boundary condition for the modified velocity $\boldsymbol{w}$ is equivalent to the no-slip condition for true velocity $\boldsymbol{v}$ on the solid walls.

The parameter ε regularly enters system (2.5)–(2.7) (in a real situation it rarely exceeds the value 10^{-2}). Furthermore, the solutions of the boundary problem (2.5)–(2.7), (2.10) (or (2.5)–(2.7), (2.11)) can be found in the form of series in terms of the powers of small parameters [22]. Then, under the expansion of the solution in terms of ε in the zero-order approximation

• with the moderate Prandtl numbers and $\varepsilon \to 0$ the microconvection system approximates the system of the viscous heat conducting fluid;

• if $\varepsilon\boldsymbol{\eta}(\tau) \to \mathbf{Ra}(\tau) \neq 0$ with $\varepsilon \to 0$, we have the Oberbeck – Boussinesq model ($\mathbf{Ra}(\tau)$ is the vector of the Rayleigh numbers).

If $\mathrm{Pr} \gg 1$, then, with the expansion of the solution in terms of Pr^{-1}
• in the limit a system of creeping motion arises:

$$\Delta \boldsymbol{w} - \nabla \bar{q} = \varepsilon \boldsymbol{\eta}(\tau)\theta, \quad \mathrm{div}\boldsymbol{w} = 0,$$
$$\theta_\tau + \boldsymbol{w} \cdot \nabla\theta + \varepsilon|\nabla\theta|^2 = (1 + \varepsilon\theta)\Delta\theta.$$

Note 4. In [37] the existence of the analytical solution with respect to ε of problem (2.1)–(2.3), (2.9) with the initial condition

$$\theta|_{t=0} = \theta^0(\boldsymbol{x}), \quad \boldsymbol{w}|_{t=0} = \boldsymbol{w}^0(\boldsymbol{x}) \quad \mathrm{div}\boldsymbol{w}^0 = 0.$$

in the Hölder's classes were proved for the microconvection in the closed domain Ω.

The solvability of the appearing initial boundary value problems in the Hölder's classes are studied in [22] when the necessary conditions of smoothness and matching are valid. The correctness of the stationary problem for the microconvection equations under conditions (2.8) and (2.9) was proved in [38].

3. Exact stationary solutions. Classification

Let the liquid fill an infinite vertical channel $\Omega = \{|x| < a, -\infty < y < \infty, -\infty < z < \infty\}$ with solid walls $x = \pm a$ (Fig. 1). At the walls, conditions (2.8) or (2.9) are specified.

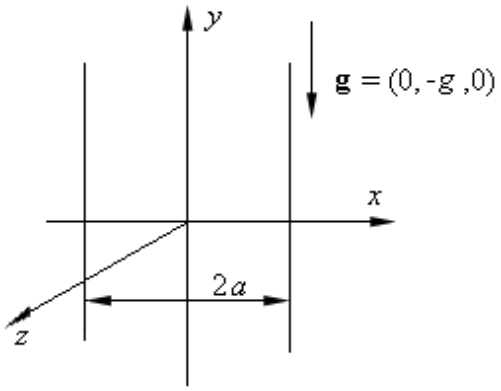

Figure 1: Flow domain.

If the temperature on the walls θ_w and value of the heat flux d do not depend on z, then, plane flows are possible in a vertical layer. The flows are realized when the initial distributions of the velocity and temperature do not depend on z and the velocity component $v_3 = 0$ with $t = 0$.

In the present paper only stationary flows will be considered.

In the plane case, the system of equations (2.1)–(2.3) for the stationary flow ($\boldsymbol{w}_t = 0, \theta_t = 0$) admits the operators $\partial/\partial y$ and $\psi\partial/\partial q$. It means that the system is invariant with regard to the transition transformation along the axis y and addition of an arbitrary constant ψ to the pressure analogue q. The invariant solution of system (2.1)–(2.3) with regard to the operator $\partial/\partial y + \psi\partial/\partial q$ can be presented in the form [20]

$$\boldsymbol{w} = (u(x), v(x), 0), \quad \theta = \theta(x), \quad q = (\varphi - g)y + r(x), \tag{3.1}$$

where $\varphi = \psi + g$, $\varphi = \text{const}$, $g = \text{const}$ is the gravity acceleration. The term $-gy$ in the expression for q corresponds to the hydrostatic component in the formula for the true pressure p. After the substitution of (3.1) into (2.1)–(2.3) the system is separated into the sequence of equations for the functions $u(x)$, $v(x)$, $\theta(x)$, $r(x)$ and constant φ.

Continuity equation (2.1) implies that $u(x) = \text{const}$ and $v(x)$ is an arbitrary function. Let $u(x) = u_0 = \text{const}$.

Taking into account (3.1) energy equation (2.3) takes the form

$$(u_0 + \beta\chi\theta_x)\theta_x = (1 + \beta\theta)\chi\theta_{xx}.$$

The last equation of the second order has a two-parameter family of stationary solutions

$$\theta(x) = \frac{1}{\beta}\left[\frac{1}{b_1} - 1 + b_2 \exp\left(\frac{b_1 u_0 x}{\chi}\right)\right], \quad b_1, b_2 = \text{const}, \quad b_1 \neq 0, \tag{3.2}$$

and an extra solution

$$\theta_0(x) = \bar{\theta} - \frac{u_0 x}{\beta\chi}, \quad \bar{\theta} = \text{const}. \tag{3.3}$$

The projection of (2.2) on the axis x leads to $(1+\beta\theta)(-r_x) = 0$. It follows that $r = \text{const}$. The function $q(x, y)$ is defined up to a constant, then, we can set $r \equiv 0$.

Linear distribution of temperature. According to (3.3) we have $u_0 + \beta\chi\theta_{0x} = 0$, then the projection of (2.2) on the axis y results in the following equation

$$\left(1 + \beta\bar{\theta} - \frac{u_0 x}{\chi}\right)(\nu v_{xx} - \varphi) + \beta\bar{\theta}g - \frac{u_0 g}{\chi}\,x = 0, \tag{3.4}$$

where φ is the unknown constant.

Three conditions are necessary to the unique definiteness of $v(x)$. Since $\bigtriangledown\theta = (\theta_{0x}, 0)$ from (2.8) we have

$$v(x) = 0, \quad x = \pm a. \tag{3.5}$$

We interpret solution (3.1) as approximately describing the convection in the central part of the finite, but quite long as compared to the width $2a$, closed region. We impose the condition of zero mass flow rate across any transversal cross-section of the layer $y = \text{const}$. Taking into account the state equation used in the microconvection model (see Note 1) we obtain

$$\int_{-a}^{a} \frac{v(x)}{1 + \beta\theta(x)}\,dx = 0. \tag{3.6}$$

The temperature distribution (3.3) is used as $\theta(x)$ in (3.6). The general solution of equation (3.4) has the form

$$v = \frac{1}{\nu}\left[(\varphi - g)\frac{x^2}{2} + c_1 x + c_2 + \frac{g\chi^2}{u_0^2}\left(1 + \beta\bar{\theta} - \frac{u_0 x}{\chi}\right)\times\right.$$
$$\left.\times\left(\ln(1 + \beta\bar{\theta} - \frac{u_0 x}{\chi}) - 1\right)\right] \tag{3.7}$$

with the arbitrary constants c_1, c_2, which are defined in (3.5):

$$\begin{aligned} c_1 &= -\frac{g\chi^2}{2au_0^2}\left(f_1 \ln f_1 - f_2 \ln f_2 + 2\frac{u_0 a}{\chi}\right), \\ c_2 &= \frac{(g - \varphi)}{2}\,a^2 - \frac{g\chi^2}{2u_0^2}\left[f_1 \ln f_1 + f_2 \ln f_2 - 2(1 + \beta\bar{\theta})\right]. \end{aligned} \tag{3.8}$$

Here, the notations $f_1 = 1 + \beta\bar{\theta} - u_0 a/\chi$, $f_2 = 1 + \beta\bar{\theta} + u_0 a/\chi$ are used.

The substitution of (3.7) into (3.6) results in

$$\varphi = g\left\{1 - \left[\frac{\chi}{2u_0 a}(\ln f_2 - \ln f_1)\Big(f_1\ln f_1 + f_2\ln f_2 + \right.\right.$$

$$\left.\left. + \frac{\chi}{u_0 a}\,(1+\beta\bar\theta)(f_1\ln f_1 - f_2\ln f_2)\Big) + 2\right] \times \right.$$

$$\left. \times \left[(1+\beta\bar\theta) + (\ln f_2 - \ln f_1)\left(\frac{u_0 a}{2\chi} - \frac{\chi}{2u_0 a}(1+\beta\bar\theta)^2\right)\right]^{-1}\right\}. \qquad (3.9)$$

In obtaining the last relation we took into account (3.8).

Thus, in the case of the linear temperature distribution the stationary solution (3.1) has the form

$$\boldsymbol{w} = (u_0, v(x), 0), \quad \theta = \bar\theta - u_0 x/\beta\chi, \quad q = (\varphi - g)y, \qquad (3.10)$$

where $v(x)$ is defined from (3.7), φ is found from (3.9) and $\bar\theta$, u_0 are calculated depending on the boundary conditions.

If the temperatures θ_1 and θ_2 are imposed at the walls $x = -a$ and $x = a$, respectively, (the Dirichlet condition (2.8)), then, we have $\theta_1 = \bar\theta + u_0 a/(\beta\chi)$, $\theta_2 = \bar\theta - u_0 a/(\beta\chi)$ from (3.3). And extra solution (3.3) will satisfy these conditions, if the constants u_0 and $\bar\theta$ depend on θ_1, θ_2 as follows

$$\bar\theta = \frac{\theta_1 + \theta_2}{2}\,, \quad u_0 = \frac{(\theta_1 - \theta_2)\beta\chi}{2a}\,. \qquad (3.11)$$

Here, the density is positive ($\beta\bar\theta > -1$) and $\theta > 0$ in the layer $|x| < a$.

If the Neumann conditions from (2.9) are imposed on the temperature function with $x = \pm a$, then, for solution (3.3) the following relation will be valid

$$\theta_x = -u_0/(\beta\chi) \equiv d/k. \qquad (3.12)$$

The temperature field (3.3) fulfills this condition with the arbitrary constant $\bar\theta$, and besides, the form of solution (3.3) imposes restrictions on the values of the heat fluxes $d|_{x=-a} = d_1$ and $d|_{x=a} = d_2$. The values d_1 and d_2 can not be arbitrary and $d_1 = d_2 = d$. It means that equal heat fluxes are supplied (or taken away depending on the sign of d) at the walls. Thus, if solution (3.10) describes the stationary flow in the vertical channel at the given equal heat fluxes at the solid walls (boundary conditions (3.12)), then, we have $u_0 = -\beta\chi d/k$.

So, in the term of true (physical) functions we can give the following physical interpretation of solution (3.10): it describes a combined flow in the vertical layer with impenetrable boundaries. The flow is characterized by the non-solenoidal velocity field, linear distribution of the temperature crosswise of the layer and zero integral heat flux on the boundary. Convective circulation occurs in the channel. The liquid rises near the heated wall and falls near the cold one. The flow consists of two opposite convective fluxes. In this case non-Boussinesq effects make oneself evident in the fact that in the channel a transversal motion induced by a constant horizontal temperature gradient is formed, i. e. the temperature drop "deforms" the longitudinal velocity field defined by formula (3.7).

Let $v_n = -\nu/(ga^2)v$ be the non-dimensional velocity, $\varepsilon = \beta\bar{\theta}$, $\mathrm{Pe} = u_0 a/\chi$ is the Peclet number, which is the ratio of the heat transferred by convection to the heat transferred by thermal conductivity. In the non-dimensional form, from (3.7) we have

$$v_n(\zeta) = -\frac{\nu}{ga^2}\,v = \frac{p_1}{4p_2\mathrm{Pe}}\,\zeta^2 - \frac{p_3}{2\mathrm{Pe}^2}\,\zeta + \frac{p_1}{4p_2\mathrm{Pe}} -$$

$$-\frac{p_4}{2\mathrm{Pe}^2} + \frac{1+\varepsilon-\mathrm{Pe}\,\zeta}{\mathrm{Pe}^2}\,[\ln(1+\varepsilon-\mathrm{Pe}\,\zeta)-1].$$

The following notations are introduced

$$p_1 = (\ln f_2^* - \ln f_1^*)\Big[f_1^*\ln f_1^* + f_2^*\ln f_2^* + \frac{1+\varepsilon}{\mathrm{Pe}}\,(f_1^*\ln f_1^* - f_2^*\ln f_2^*)\Big] + 4\mathrm{Pe},$$

$$p_2 = 1+\varepsilon + (\ln f_2^* - \ln f_1^*)\Big(\frac{\mathrm{Pe}}{2} - \frac{(1+\varepsilon)^2}{2\mathrm{Pe}}\Big),$$

$$p_3 = f_1^*\ln f_1^* - f_2^*\ln f_2^* + 2\mathrm{Pe}, \quad p_4 = f_1^*\ln f_1^* + f_2^*\ln f_2^* - 2(1+\varepsilon),$$

$$f_1^* = 1+\varepsilon-\mathrm{Pe}, \quad f_2^* = 1+\varepsilon+\mathrm{Pe}.$$

Note 5. It is easy to show that solution (3.10) with $\varepsilon \to 0$ approximates the known solution of the stationary problem in the Oberbeck – Boussinesq model [39]

$$v_b = \frac{\mathrm{Ra}}{6}\,(\zeta - \zeta^3), \quad p_b = \bar{p} - \rho_1 ga\xi\ (\xi = y/a), \quad \theta_b = -\theta_1\zeta,$$

where $\bar{p} = \mathrm{const}$ is the pressure deviation from the hydrostatic one. Differences appear in the distribution of the vertical velocity component. The

function v_n in the microconvection model loses the property of being odd which is inherent to the velocity function v_b in the Oberbeck – Boussinesq model.

If $\theta_1 = \theta_2$ then, the temperature in the layer will be constant, $\theta(x) = \theta_1$, and according to (3.11), $u_0 = 0$. In this case, the flow in the vertical channel is a unidirectional one and the motion is generated by the pressure drop. The distribution of the vertical velocity has the form

$$v(x) = \Big(\frac{\varphi}{\nu} - \frac{\beta\theta_1 g}{\nu(1+\beta\theta_1)}\Big)\Big(\frac{x^2}{2} - \frac{a^2}{2}\Big). \tag{3.13}$$

The value φ is defined from the condition of nonzero mass flow rate

$$\int\limits_{-a}^{a} \frac{\rho_0 v(x)}{1+\beta\theta_1}\, dx = m \neq 0$$

and it equal to

$$\varphi = \frac{\beta\theta_1 g}{1+\beta\theta_1} - \frac{3m\nu(1+\beta\theta_1)}{2\rho_0 a^3}\,. \tag{3.14}$$

In this case the stationary solution

$$\boldsymbol{w} = (0, v(x), 0), \qquad \theta = \theta_1 = \text{const}, \qquad q = (\varphi - g)y \tag{3.15}$$

describes the forced plane-parallel isothermal flow in the channel with the solid impermeable boundaries. The flow is induced by non-zero pressure gradient. In (3.15) the function $v(x)$ is defined by (3.13), φ is found from (3.14). Here, both classes of the boundary conditions for the temperature function can be imposed formally. If the Dirichlet condition for the temperature function from (2.8) is used, then, the equality $\theta_1 = \theta_2$ must be fulfilled. If the Neumann condition from (2.9) is applied, then $d_1 = d_2 = 0$ must be satisfied. Deformation of the velocity field does not appear, since there is no any action of the thermal effects.

Let us introduce the specified Reynolds number $\mathrm{Re}_m = m/(\rho_0\chi)$. Now, taking into account (2.4) the non-dimensional velocity is $v_n = av/\chi$, and in non-dimensional variables, expression (3.13) takes the form

$$v_n(\zeta) = -\frac{3}{2}\,\mathrm{Re}_m(1+\varepsilon)\Big(\frac{\zeta^2}{2} - \frac{1}{2}\Big).$$

Exponential distribution of temperature. Let the following conditions be valid

$$\frac{1}{\beta}\left[\frac{1}{b_1}-1+b_2\exp\left(-\frac{b_1u_0a}{\chi}\right)\right]=\theta_1,\ \frac{1}{\beta}\left[\frac{1}{b_1}-1+b_2\exp\left(\frac{b_1u_0a}{\chi}\right)\right]=\theta_2 \tag{3.16}$$

for stationary solution (3.2). If we subtract the first equation of system (3.16) from the second one we will obtain

$$\frac{b_2}{\beta}=\frac{\theta_2-\theta_1}{\exp(\mu)-\exp(-\mu)}\,, \tag{3.17}$$

where $\mu = b_1u_0a/\chi$.

The following possible variants will be considered:

1. If $\theta_1 = \theta_2$, then $b_2 = 0$ and $b_1 = 1/(1+\beta\theta_1)$, i.e. the temperature in the layer is constant and $\theta_x = 0$. The equality $u_0 = 0$ follows from the condition for the horizontal component of the velocity $u_0 + \beta\chi\theta_x = 0$. Then,this solution coincides with (3.15).

2. Let $\theta_1 \neq \theta_2$. Then, substitute (3.17) into the first equation (3.16), and introduce new variables

$$\omega=\frac{\beta\chi(\theta_2-\theta_1)}{u_0a}\,,\quad \sigma=(1+\beta\theta_1)\frac{\chi}{u_0a}.$$

Then, we obtain the following equation

$$\frac{1}{\mu}+\frac{\omega}{\exp(2\mu)-1}=\sigma. \tag{3.18}$$

The analysis of equation (3.18) was performed in [28]. In the last work the existence of a unique solution μ_1 was proved and constants b_1, b_2 were defined:

$$b_1=\frac{\chi}{u_0a}\,\mu_1>0,\quad b_2=\frac{2\beta(\theta_2-\theta_1)}{\mathrm{sh}\mu_1}\,. \tag{3.19}$$

The projection of (2.2) on the axis y, taking into account (3.2) and (3.19), results in an equation for determining the vertical component of the velocity v

$$\left(\frac{1}{b_1}+b_2\exp(b_3x)\right)\nu v_{xx}-b_1b_2u_0\exp(b_3x)v_x=f(x), \tag{3.20}$$

where

$$b_3=\frac{b_1u_0}{\chi}\,,\quad f(x)=\varphi\left(\frac{1}{b_1}+b_2\exp(b_3x)\right)-g\left(\frac{1}{b_1}-1+b_2\exp(b_3x)\right).$$

After changing $z = 1+b_1b_2\exp(b_3x)$ the general solution of equation (3.20) has the form

$$v = \int\limits_{h_1}^{z} \frac{z^\alpha}{z-1}\left[\frac{\varphi-g}{\nu b_3^2}\int \frac{dz}{z^\alpha(z-1)} + \frac{gb_1}{\nu b_3^2}\int \frac{dz}{z^{\alpha+1}(z-1)} + D_1\right] dz + D_2, \tag{3.21}$$

$D_1, D_2 = \text{const}$, $h_1 = 1 + b_1b_2\exp(-\gamma_1)$, $\gamma_1 = ab_3$, $\alpha = \chi/\nu \equiv 1/\text{Pr}$.

The constant φ is defined from (3.6)

$$\varphi = g(1 - b_1F_1) - D_1\nu b_3^2F_2, \tag{3.22}$$

where

$$F_1 = \frac{\displaystyle\int\limits_{h_1}^{h_2}\frac{1}{z}\int\limits_{h_1}^{z}\frac{\sigma^\alpha}{\sigma-1}\int\limits_{h_1}^{\sigma}\frac{d\tau}{\tau^{\alpha+1}(\tau-1)}\,d\sigma dz}{\displaystyle\int\limits_{h_1}^{h_2}\frac{1}{z}\int\limits_{h_1}^{z}\frac{\sigma^\alpha}{\sigma-1}\int\limits_{h_1}^{\sigma}\frac{d\tau}{\tau^{\alpha}(\tau-1)}\,d\sigma dz},$$

$$F_2 = \frac{\displaystyle\int\limits_{h_1}^{h_2}\frac{1}{z}\int\limits_{h_1}^{z}\frac{\sigma^\alpha}{\sigma-1}\,d\sigma dz}{\displaystyle\int\limits_{h_1}^{h_2}\frac{1}{z}\int\limits_{h_1}^{z}\frac{\sigma^\alpha}{\sigma-1}\int\limits_{h_1}^{\sigma}\frac{d\tau}{\tau^{\alpha}(\tau-1)}\,d\sigma dz},$$

$h_2 = 1 + b_1b_2\exp(\gamma_1)$. The integration constants D_1, D_2 are found from the no-slip conditions at the immovable solid walls

$$D_1 = \frac{\dfrac{gb_1F_1}{\nu b_3^2}\displaystyle\int\limits_{h_1}^{h_2}\frac{z^\alpha}{z-1}\int\limits_{h_1}^{z}\frac{d\sigma}{\sigma^\alpha(\sigma-1)}\,dz - \frac{gb_1}{\nu b_3^2}\int\limits_{h_1}^{h_2}\frac{z^\alpha}{z-1}\int\limits_{h_1}^{z}\frac{d\sigma}{\sigma^{\alpha+1}(\sigma-1)}\,dz}{\displaystyle\int\limits_{h_1}^{h_2}\frac{z^\alpha}{z-1}\,dz - F_2\int\limits_{h_1}^{h_2}\frac{z^\alpha}{z-1}\int\limits_{h_1}^{z}\frac{d\sigma}{\sigma^\alpha(\sigma-1)}\,dz}, \quad D_2 = 0.$$

As regards a physical interpretation in the last case, the solution

$$\boldsymbol{w} = (u_0, v(x), 0), \qquad \theta = \theta(x), \qquad q = (\varphi - g)y, \tag{3.23}$$

with $v(x)$ from (3.21), φ from (3.22) and $\theta(x)$ from (3.2), provides a description of the nonisothermal flow in the channel with the impermeable boundaries. The flow is characterized by the non-solenoidal velocity field, exponential distribution of the temperature crosswise of the layer and zero integral heat flux on the boundary. As before, non-Boussinesq effects are related to the influence of the nonuniformity of temperature field. They lead to deformation of the longitudinal velocity.

It can be shown that for the temperature function of solution (3.23) the Neumann condition from (2.9) can not be used. Actually, let conditions (2.9) be imposed at the channel walls. Then, for solution (3.2) the constants b_1 and b_2 are equal to

$$b_1 = \frac{\chi}{2u_0 a} \ln\frac{d_2}{d_1}, \quad b_2 = \frac{2\beta d_1 a\sqrt{d_2}}{k\sqrt{d_1}\ln(d_2/d_1)}$$

respectively. It is obvious that for solution (3.2) to exist it is required that $d_1 \neq d_2$. But the condition for the horizontal component of the velocity $u_0 + \beta\chi\theta_x = 0$ leads to the equality $d_1 = d_2$. Thus, for the temperature function $\theta(x)$ of solution (3.23) only the Dirichlet condition can be used.

Rewrite expression (3.21) in the non-dimensional form

$$v_n(\zeta) = \frac{\nu b_3^2}{g} v, \quad -1 \le \zeta \le 1,$$

where

$$v(\zeta) = -(b_1F_1 + D_1^*F_2)\gamma_1^2 \int_{-1}^{\zeta} (1 + b_1b_2\exp(\gamma_1\zeta))^\alpha \int \frac{d\sigma}{(1 + b_1b_2\exp(\gamma_1\sigma))^\alpha}\, d\zeta +$$

$$+b_1\gamma_1^2 \int_{-1}^{\zeta} (1 + b_1b_2\exp(\gamma_1\zeta))^\alpha \int \frac{d\sigma}{(1 + b_1b_2\exp(\gamma_1\sigma))^{\alpha+1}}\, d\zeta +$$

$$+D_1^* \int_{-1}^{\zeta} (1 + b_1b_2\exp(\gamma_1\zeta))^\alpha d\zeta,$$

$$D_1^* = \left(b_1F_1\gamma_1^2 \int_{-1}^{1} (1 + b_1b_2\exp(\gamma_1\zeta))^\alpha \int_{-1}^{\zeta} \frac{d\sigma}{(1 + b_1b_2\exp(\gamma_1\sigma))^\alpha}\, d\zeta -\right.$$

$$-b_1\gamma_1^2\int\limits_{-1}^{1}(1+b_1b_2\exp(\gamma_1\zeta))^{\alpha}\int\limits_{-1}^{\zeta}\frac{d\sigma}{(1+b_1b_2\exp(\gamma_1\sigma))^{\alpha+1}}\,d\zeta\Bigg)\times$$

$$\times\Bigg(\gamma_1\int\limits_{-1}^{1}(1+b_1b_2\exp(\gamma_1\zeta))^{\alpha}\,d\zeta-$$

$$-F_2\gamma_1^2\int\limits_{-1}^{1}(1+b_1b_2\exp(\gamma_1\zeta))^{\alpha}\int\limits_{-1}^{\zeta}\frac{d\sigma}{(1+b_1b_2\exp(\gamma_1\sigma))^{\alpha}}\,d\zeta\Bigg)^{-1}.$$

Note 6. With Pe $\to$ 0 the temperature field (3.2) approximates the linear profile (3.3) regardless of the type of the boundary condition [32].

Classification of solutions. Solution (3.1) describes different classes of the stationary flows. The flow type depends on the values of the problem parameters and boundary condition for the temperature function. In the terms of true physical characteristics the following classification of the flow types is proposed:

Flow 1 is the convective flow in the layer with the impenetrable walls with a transversal uniform stream ($u_0 \neq 0$), caused by the non-Boussinesq effects, and linear profile of the temperature (3.3). Both classes of the boundary conditions for the temperature functions can be imposed. If the second-type boundary conditions are used the restriction on the values of the heat fluxes will arise. The values of the heat fluxes at the walls must be equal.

Flow 2 is the unidirectional ($u_0 = 0$) isothermal flow in the layer with the impermeable walls with the velocity (3.13), induced by the action of the pressure gradient. Both classes of the boundary conditions for the temperature function can formally be used. The temperatures θ_1 and θ_2 at the walls must be equal in the Dirichlet conditions. The heat fluxes d_1 and d_2 at the walls must be equal to zero in the Neumann conditions.

Flow 3 is the convective flow in the layer with the impenetrable walls with a transversal uniform stream ($u_0 \neq 0$), caused by the non-Boussinesq effects, and exponential distribution of the temperature (3.2). Only the first-type boundary conditions for the temperature function can be imposed at the walls.

In Fig.2 typical velocity fields and distribution of the vertical component of the velocity (solid line) for the model medium (silicon dioxide melt) are presented. The following values of the physical parameters are used: $\nu =$

$2.65 \cdot 10^{-3}$ cm^2/s, $\chi = 0.49$ cm^2/s, $\beta = 0.75 \cdot 10^{-5}\,{}^o\mathrm{C}^{-1}$, $\rho_0 = 1.9$ g/cm^3. One can see the deformation of the velocity field induced by the presence of the non-zero transversal component of the velocity (Fig. 2, a, c).

The non-linearity of the microconvection equations is the reason for the non-uniqueness of the admitted exact solutions. These solutions are essentially different, therefore, it is important to define the stability boundaries of all the existing regimes.

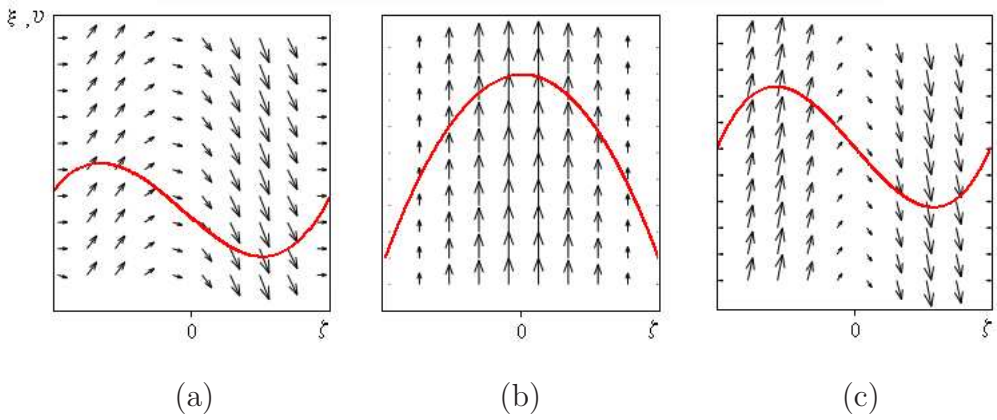

(a) (b) (c)

Figure 2: Typical velocity fields and distribution of the longitudinal component of the velocity (solid line) in the vertical layer: a) — *Flow 1*, $v = v_n \cdot 10^2$, $\varepsilon = 0.01$, Pe $= 0.002$; b) — *Flow 2*, $v = v_n \cdot 10^3$, $\varepsilon = 0.01$, $\mathrm{Re}_m = 0.655$; c) — *Flow 3*, $v = v_n \cdot 10^3$, $\varepsilon = 0.01$, Pe $= 0.002$.

4. Equations of small disturbances

Let $\tilde{w}(\boldsymbol{x},t) = \boldsymbol{w}(\boldsymbol{x},t) + \boldsymbol{W}(\boldsymbol{x},t)$, $\tilde{q}(\boldsymbol{x},t) = q(\boldsymbol{x},t) + Q(\boldsymbol{x},t)$, $\tilde{\theta} = \theta(\boldsymbol{x},t) + T(\boldsymbol{x},t)$, where $\boldsymbol{W} = (U,V,W)$, Q, T are the perturbations of the velocity, pressure and temperature, respectively, $\boldsymbol{w}(\boldsymbol{x},t) = (u,v,w)$, $q(\boldsymbol{x},t)$, $\theta(\boldsymbol{x},t)$ is the basic solution. The functions $\tilde{w}, \tilde{q}, \tilde{\theta}$ are the solutions of the boundary-value problem (2.1)–(2.3), (2.8).

The linearized equations for the small perturbations in the non-dimensional variables have the following form

$$U_\tau + \mathrm{Pe}\, U_\zeta + vU_\xi - \varepsilon v_\zeta T_\xi + \varepsilon^2 \theta_\zeta (T_{\xi\xi} + T_{\vartheta\vartheta}) = (1+\varepsilon\theta)(-Q_\zeta + \Delta U)\mathrm{Pr},$$

$$V_\tau + \mathrm{Pe}\, V_\zeta + vV_\xi + v_\zeta U + \varepsilon[\theta_\zeta (V_\zeta - U_\xi) + v_\zeta T_\zeta] +$$

$$+\varepsilon^2(\theta_{\zeta\zeta}T_\xi - \theta_\zeta T_{\zeta\xi}) = (1+\varepsilon\theta)(-Q_\xi + \Delta V)\mathrm{Pr} + \frac{\mathrm{Gr}\,T}{1+\varepsilon\theta}\,, \tag{4.1}$$

$$W_\tau + \mathrm{Pe}\,W_\zeta + vW_\xi + \varepsilon\theta_\zeta(W_\zeta - U_\vartheta) + \varepsilon^2(\theta_{\zeta\zeta}T_\vartheta - \theta_\zeta T_{\zeta\vartheta}) =$$

$$= (1+\varepsilon\theta)(-Q_\vartheta + \Delta W)\mathrm{Pr},$$

$$U_\zeta + V_\xi + W_\vartheta = 0,$$

$$T_\tau + \mathrm{Pe}\,T_\zeta + vT_\xi + \theta_\zeta U + 2\varepsilon\theta_\zeta T_\zeta = (1+\varepsilon\theta)\Delta T + \varepsilon\theta_{\zeta\zeta}T$$

with $-1 < \zeta < 1$, $-\infty < \xi < \infty$, $-\infty < \vartheta < \infty$ with the boundary conditions

$$\boldsymbol{W} + \varepsilon\nabla T = 0, \quad T = 0, \quad |\zeta| = 1, \tag{4.2}$$

where $\varepsilon = \beta\bar{\theta}$, $\mathrm{Gr} = \beta\bar{\theta}ga^3/\chi^2 = \varepsilon\eta\mathrm{Pr}$.

We will find a solution of boundary problem (4.1), (4.2) in the form of normal modes

$$(\boldsymbol{W}, Q, T) = (\boldsymbol{W}(\zeta), Q(\zeta), T(\zeta)) \cdot \exp\left[i(\alpha_1\xi + \alpha_2\vartheta - \mathrm{C}\tau)\right], \tag{4.3}$$

where α_1, α_2 are the wave numbers along the ξ, ϑ axes, respectively. In the common case, C is the complex number $\mathrm{C} = C_r + iC_i$. The perturbations are propagated in the flux in waves at an angle $\phi = \alpha_1/\alpha_2$ in the direction of the axis ξ with common wave number $\alpha = \sqrt{\alpha_1^2 + \alpha_2^2}$ and phase velocity $\omega = C_r/\alpha$. Fading out or growing perturbations are defined by the sign of the imaginary part C_i, the value C_r specifies the frequency of oscillations. If the decrement C is a pure imaginary number, then with $C_i < 0$ the perturbations will fade out monotonically; with $C_i > 0$ the perturbations will grow monotonically. The conditions $C_i(M, \alpha) = 0$, $C_r(M, \alpha) = 0$ define the boundaries of the stability with regard to the monotonic and oscillatory perturbations, respectively. Here, M is a set of the known parameters of the problem.

For the perturbations of the normal modes type the analogue of the Squire transformation exists [33]

$$\widetilde{Z} = i\alpha_1 V + i\alpha_2 W, \quad \widetilde{U} = i\alpha U, \quad \widetilde{Q} = i\alpha Q, \quad \widetilde{T} = i\alpha T, \tag{4.4}$$

which allows one to reduce the problem with regard to the three-dimensional perturbations (4.3) to the corresponding plane problem [33]

$$i(\alpha\lambda v - \mathrm{C})\widetilde{Z} + (\mathrm{Pe} + \varepsilon\theta_\zeta)\widetilde{Z}_\zeta + (\lambda v_\zeta - i\alpha\,\varepsilon\theta_\zeta)\widetilde{U} + (\varepsilon\lambda v_\zeta - i\alpha\varepsilon^2\theta_\zeta)\widetilde{T}_\zeta +$$

$$+ i\alpha\varepsilon^2\theta_{\zeta\zeta}\widetilde{T} = (1+\varepsilon\theta)\left[-i\alpha\widetilde{Q} + \widetilde{Z}_{\zeta\zeta} - \alpha^2\widetilde{Z}\right]\mathrm{Pr} + \frac{\lambda\mathrm{Gr}\,\widetilde{T}}{1+\varepsilon\theta}\,, \tag{4.5}$$

$$i(\alpha\lambda v - \mathrm{C})\widetilde{U} + \mathrm{Pe}\,\widetilde{U}_\zeta - [i\alpha\,\varepsilon\,\lambda v_\zeta + \varepsilon^2\theta_\zeta\alpha^2]\widetilde{T} =$$
$$= (1+\varepsilon\theta)[-\widetilde{Q}_\zeta + \widetilde{U}_{\zeta\zeta} - \alpha^2\widetilde{U}]\mathrm{Pr}, \tag{4.6}$$

$$\widetilde{U}_\zeta + i\alpha\widetilde{Z} = 0, \tag{4.7}$$

$$i(\alpha\lambda v - \mathrm{C})\widetilde{T} + (\mathrm{Pe} + 2\varepsilon\theta_\zeta)\widetilde{T}_\zeta + \theta_\zeta\widetilde{U} = (1+\varepsilon\theta)[\widetilde{T}_{\zeta\zeta} - \alpha^2\widetilde{T}] + \varepsilon\theta_{\zeta\zeta}\widetilde{T}. \tag{4.8}$$

System (4.5)–(4.8) contains an additional parameter $\lambda = \alpha_1/\alpha$, which characterizes spatial perturbations and can have the values belonging to the segment $[0, 1]$. The value $\lambda = 0$ corresponds to the perturbations with $\alpha_1 = 0$, which do not depend on the longitudinal coordinate ξ and are periodical with respect to ϑ. These perturbations are not the plane ones, since in this case the component $V \neq 0$. In the stationary regime the liquid particles move along helix lines, whose axes are parallel to the direction of the basic motion (the so-called "spiral" perturbations). Another limiting case is $\lambda = 1$, which corresponds to the plane perturbations with $\alpha_2 = 0$.

Furthermore, the functions $\widetilde{U}, \widetilde{Z}, \widetilde{T}$, defined by relations (4.4), satisfy the boundary conditions which are equivalent to (4.2):

$$|\zeta| = 1: \qquad \widetilde{U} + \varepsilon\widetilde{T}_\zeta = 0, \quad \widetilde{Z} = 0, \quad \widetilde{T} = 0. \tag{4.9}$$

Boundary problem (4.5)–(4.9) specifies the perturbations and their decrements C, depending on the parameters α, λ, ε, Pe, Pr and Gr. The parameter λ is to be a fixed one to calculate the characteristics of the spatial perturbations using the solution of the plane problem (4.5)–(4.9).

5. Spectrum of perturbations

The problem of the stability of isothermal *Flow 2* with regard to the "spiral" perturbations is solved analytically. Actually, in this case $\lambda = 0$, $\theta_\zeta = 0$, $\theta_{\zeta\zeta} = 0$, Pe $= 0$, and equations (4.5)–(4.8) are greatly simplified. It is clear that the basic flow does not interact with the perturbations in the form of the longitudinal rolls with $\lambda = 0$. Therefore, the critical Grashof number of the mode does not depend on the specified Reynolds number, characterizing the intensity of the hydrodynamic flow.

The spectrum of the eigenvalues is defined from the Sturm – Liouville problem for the temperature perturbations

$$\widetilde{T}'' + \frac{i\mathrm{C} - (1+\varepsilon\theta_1)\alpha^2}{1+\varepsilon\theta_1}\widetilde{T} = 0, \quad \widetilde{T}(-1) = \widetilde{T}(1) = 0. \tag{5.1}$$

The solution of the eigenvalue problem (5.1) is known [40]. The coefficient of $\widetilde{T}$ determines the spectrum of the eigenvalues

$$\frac{i\mathrm{C}_n - (1+\varepsilon\theta_1)\alpha^2}{1+\varepsilon\theta_1} = \frac{\pi^2 n^2}{4}, \quad n = 1, 2, ...$$

It follows that

$$C_n = -i\Big(\frac{\pi^2 n^2}{4} + \alpha^2\Big)(1+\varepsilon\theta_1), \quad n = 1, 2, ... \tag{5.2}$$

One can see from (5.2) that all the eigenvalues are pure imaginary numbers with the negative imaginary part. It means that the "spiral" perturbations monotonically damp. The corresponding eigenfunctions defining the spectrum of the characteristic temperature perturbations have the form $\widetilde{T}_n = \sin(\pi n(\zeta+1)/2)$.

The problem for the characteristic velocity perturbations is split into a sequence of the problems for the functions $\widetilde{U}$ and $\widetilde{Z}$. If we eliminate $\widetilde{Q}$ from equations (4.5), (4.6) and express $\widetilde{Z}$ using (4.7), the analogue of the Orr – Sommerfeld equation for $\widetilde{U}$ can be obtained

$$\mathrm{C}(\widetilde{U}'' - \alpha^2\widetilde{U}) = (1+\varepsilon\theta_1)(i\widetilde{U}^{(IV)} - 2i\alpha^2\widetilde{U}'' + i\alpha^4\widetilde{U})\mathrm{Pr}$$

with the boundary conditions

$$|\zeta| = 1: \qquad \widetilde{U} + \varepsilon\widetilde{T}' = 0, \quad \widetilde{U}' = 0.$$

Using the procedures described in [41] the following expression is obtained

$$\mathrm{C} = -i(1+\varepsilon\theta_1)\mathrm{Pr}\,\frac{\int\limits_{-1}^{1}|U''|^2 d\zeta + 2\alpha^2\int\limits_{-1}^{1}|U'|^2 d\zeta + \alpha^4\int\limits_{-1}^{1}|U|^2 d\zeta}{\int\limits_{-1}^{1}|U'|^2 d\zeta + \alpha^2\int\limits_{-1}^{1}|U|^2 d\zeta}.$$

It follows that the eigenvalues are again the pure imaginary numbers with the negative imaginary part. It guarantees the stability of the flow with regard to purely hydrodynamic perturbations.

In the common case, the calculation of the perturbations spectrum for the silicon dioxide melt SiO_2 ($Pr = 5.41 \cdot 10^{-3}$) is performed using the stepwise integration method with orthogonalization [42, 43] with the arbitrary $\lambda \in [0, 1]$, α, ε, Pe and Gr. In fact, for the specific model medium the variations of λ and α correspond to the changes in the configuration of the perturbations waves, Pe is connected with the transversal velocity or/and channel thickness, Gr is associated with the gravity action or/and channel thickness. The analysis of the eigenfunctions shows that the perturbations appear to be the convective structures such as small-scale cells and hydrothermal rolls. The form of these patterns depends on the problem parameters, and the spatial size is defined by the perturbation wavelength ($\lambda_w = 2\pi/\alpha$). It should be noted that except for the above mentioned "spiral" perturbations of the isothermal *Flow 2*, the formation of oscillatory regimes is possible in the system. The convective cells periodically oscillate ($C_r \neq 0$) and fade out with time ($C_i < 0$) with the physically reasonable values of the problem parameters. The growing oscillatory perturbations appear only with rather large values of ε and Pe. Such values are difficult to obtain under real conditions. The existence of the oscillatory regimes is possible due to the properties of the arising spectral problem and is connected with its non-self-conjugation.

Non-isothermal flows

Influence of the perturbation configuration. The variations of the wavelength of the perturbations and their orientation in space result in the change in the form and size of the cells. In microgravity ($\eta < 1$) the convective structures (Fig. 3, a – c; Fig. 4, a – c) appear. With the wavelength decreasing, these structures take the form of the small-scale cells (Fig. 3, b, c). The perturbation of the temperature field leads to the formation of the alternate thermal rolls (Fig. 3, d; Fig. 4, f) or "spots" (Fig. 3, e, f; Fig. 4, d). In the case of the shortwave perturbations, the pattern size is close to the size of the convective cells.

A typical feature is not only the change in the form of the cells, but also the intensity of the liquid motion in the convective structures changes with the variations of λ. It is clear that with $\lambda = 0$ the basic flow interacts with the "spiral" disturbances in the form of the longitudinal rolls only through the transversal component of the velocity (Fig. 4, a, d). With $\lambda \neq 0$ the spatial structure of the flow is complicated; here, some symmetry of the cells with respect to the longitudinal axis is retained. The disturbed motion of the liquid particles is defined by the thermal field. It is clearly seen under the formation of the small-scale thermal "spots", in this case the cells arise

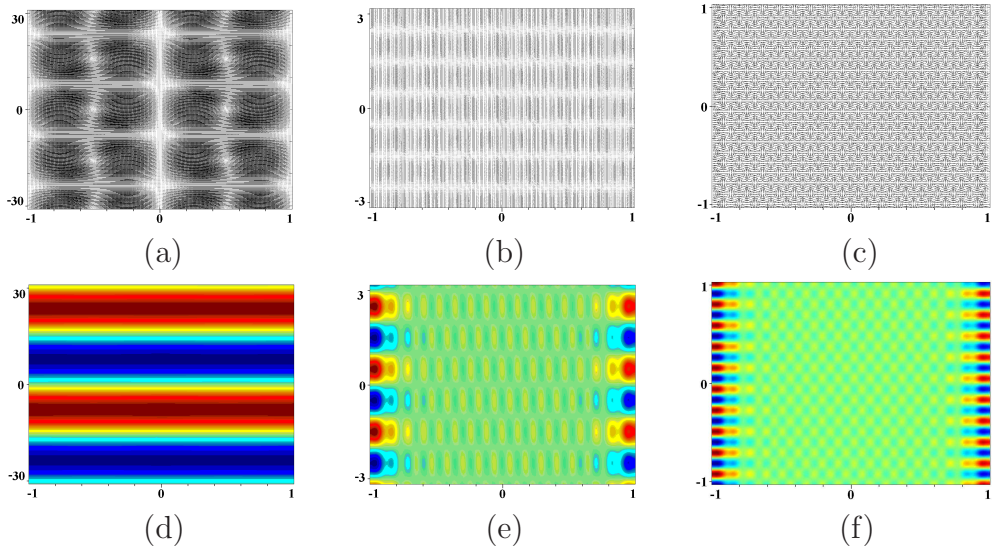

Figure 3: Distributions of the perturbations of the velocity (a – c) and temperature (d – f) of *Flow 1* with $g = g_0 \cdot 10^{-6}$, $\varepsilon = 0.01$, Pe $= 0.002$, $\lambda = 0.5$: a), d) — $\alpha = 0.2$; b), e) — $\alpha = 5$; c), f) — $\alpha = 10$.

"between" the spots.

Gravity influence. The increasing gravity action leads to the increasing sizes of the cells and thermal "spots". Furthermore, the increasing g results in the formation of the hydrothermal shafts which appear due to the interaction of the disturbances with the basic flow. The liquid particles rise along the roll axis in the direction of the hot walls and go down in the direction of the cold wall. The orientation of the rolls depends on the configuration of the perturbation wave, and the size of the rolls also depends on the gravity (Fig. 5). With the increasing g a typical buffer zone appears at the boundary of the counter currents. The velocity perturbations become weaker due to viscous effects as the particles move out of this zone (Fig. 5, c).

Influence of the temperature drop on the walls. The convective cells with intense motion are generated with the increasing temperature drop on the walls. It ensures heat transfer through the full-width channel (Fig. 6).

As a result of the interaction of the hydrodynamic and thermal perturbations, hydrothermal shafts also appear in the central part of the channel (Fig. 6, c, f). These rolls form a buffer zone, out of this area the viscous effects essentially stabilize the flow near the channel walls (Fig. 6, c). It should be noted that the value $\varepsilon = 0.05$ is difficult to obtain under real conditions.

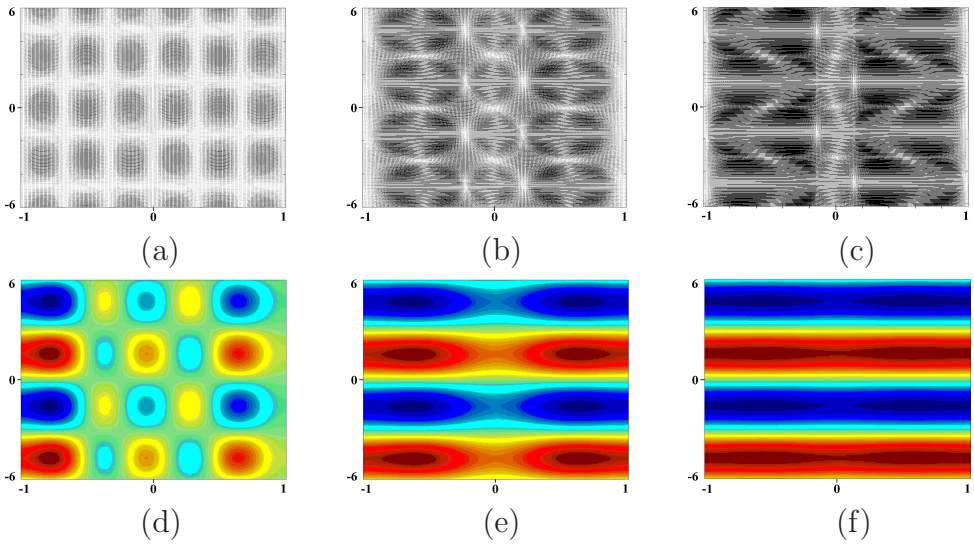

Figure 4: Distributions of the perturbations of the velocity (a – c) and temperature (d – f) of *Flow 1* with $g = g_0 \cdot 10^{-6}$, $\varepsilon = 0.01$, Pe $= 0.002$, $\alpha = 1$: a), d) — $\lambda = 0$; b), e) — $\lambda = 0.6$; c), f) — $\lambda = 1$.

For the silicon dioxide melt the temperature drop on the channel walls of about 9000 $^{\mathrm{O}}$C corresponds to this value. Due to the form of solutions (3.2) and (3.3) the growing thermal action leads to the increasing horizontal components of the velocity (see formulae (3.11) and (3.19)) and influences the distribution of the velocity disturbances.

Influence of the transversal flow velocity. The variation of the horizontal component of the velocity has little effect on the characteristics of the hydrodynamic perturbations (Fig. 7, a – c), but leads to the transformation of the thermal disturbances field. The paradoxical result is easily explained by the dependence of u_0 on the temperature characteristics (see the analysis of the solutions of the energy equation in Section 3) for the non-isothermal *Flow 1* and *Flow 3*.

Thus, the variations of the transversal velocity lead to the same changes of the perturbation fields as in the previous case (see Fig. 6 and Fig. 7). Weak dependence of the hydrodynamic characteristics on the Pe values allows one to assume the stabilizing effect of the transversal flow.

Linear size influence. In microgravity ($\eta \leq 1$) with the increasing width of the channel, the size of the convective cells (Fig. 8, a, b) and thermal "spots" (Fig. 8, d, e) changes. It is likely to be caused by the attenuation of

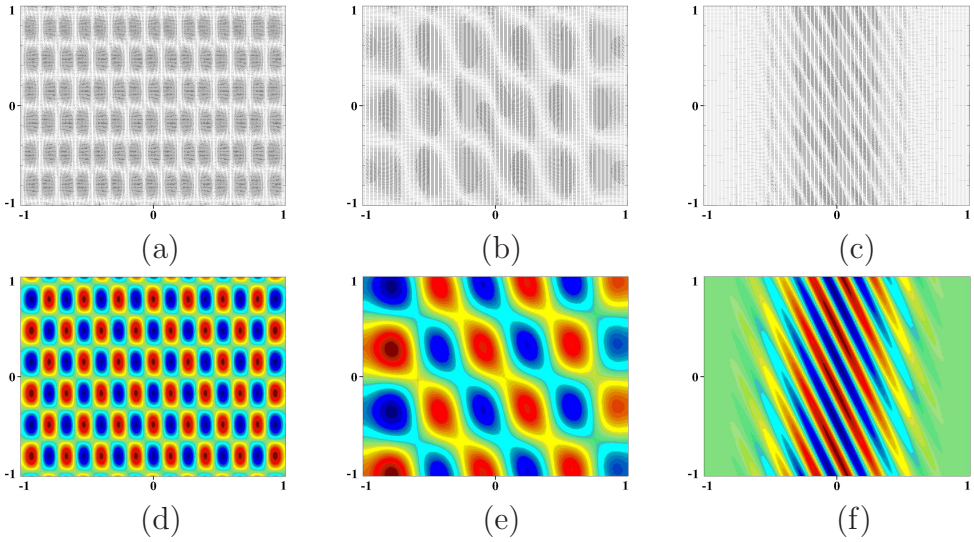

Figure 5: Distributions of the perturbations of the velocity (a – c) and temperature (d – f) of *Flow 1* with $\varepsilon = 0.01$, $\mathrm{Pe} = 0.002$, $\alpha = 10$, $\lambda = 0.2$: a), d) — $g = g_0 \cdot 10^{-6}$; b), e) — $g = g_0 \cdot 10^{-4}$; c), f) — $g = g_0 \cdot 10^{-2}$.

the viscous effects, which are significant across the full channel width in the case of the small linear sizes.

With rather large transversal sizes, when η becomes higher than 1, the hydrothermal shafts at the boundary of the counter currents are formed even in the weak gravitational field due to the heat transfer from the basic flow to the perturbations (Fig. 8, c, f). Near the channel walls the cell disturbances appear. These perturbations break with the distance from the walls.

For *Flow 3* a similar dependence of the perturbations characteristics on the problem parameters is observed. There are differences in the thermal perturbations. In this case, typical asymmetric patterns arise (Fig. 9), which are due to the non-linearity of the temperature field of the basic flow.

Isothermal flow

Influence of the perturbation configuration. The perturbations generate vortices, and the size of these swirls decreases with the wavelength decrease (Fig. 10) as well as for *Flow 1* and *Flow 3*.

All the disturbances of the isothermal *Flow 2* are monotonic ones ($C_r = 0$). The spatial perturbations can be convective structures, which take a rectangular form with the diagonal symmetry near the walls. With the distance from the walls the perturbations imply the triangular shape due to the inter-

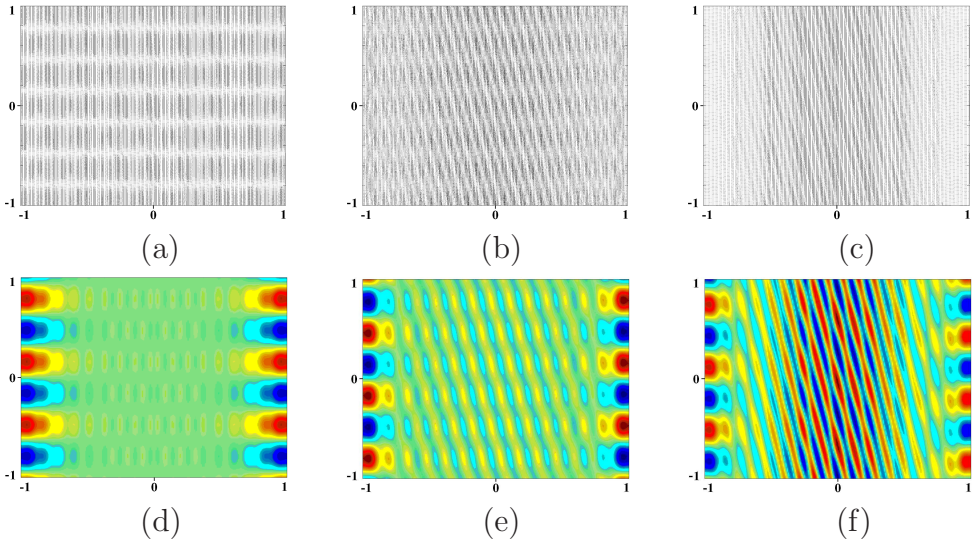

Figure 6: Distributions of the perturbations of the velocity (a – c) and temperature (d – f) of *Flow 1* with $g = g_0 \cdot 10^{-4}$, Pe = 0.002, $\alpha = 10$, $\lambda = 0.8$: a), d) — $\varepsilon = 0.001$; b), e) — $\varepsilon = 0.01$; c), f) — $\varepsilon = 0.05$.

action with the basic flow. The side boundaries of such "cells" make an angle $\pm\phi$ with the axis of the basic flow (Fig. 11, b). With the increasing λ the reconstruction of the structure shape from the polygonal form to the cellular one occurs, and besides, an area with the vortices of smaller size arises in the central part of the channel (Fig. 11, c).

Gravity influence. In a very weak gravitational field the viscous effects are essential, therefore, periodic rectangular cells elongated along the axis of the basic flow, are uniformly located across full channel width (Fig. 12, a). With the growing g a specific domain appears in the central part of the channel. In this area the cells take on a rhombic shape. On either side of the domain a complex of several vortices of irregular form arises (Fig. 12, b). If $\eta > 1$, then the formation region of the rhombic cells widens and near the walls the vortex patterns are still more deformed and decrease in size (Fig. 12, c).

Influence of the linear size or/and mass flow rate With the increasing linear size the transition from the polygonal structures having a complex form, being elongated along the axis of the basic flow (Fig. 13, a) to the cellular perturbations (Fig. 13, b) occurs. With the further increase in the channel width the rhombic cells with a marked chessboard structure are formed in the central part of the channel (Fig. 13, c).

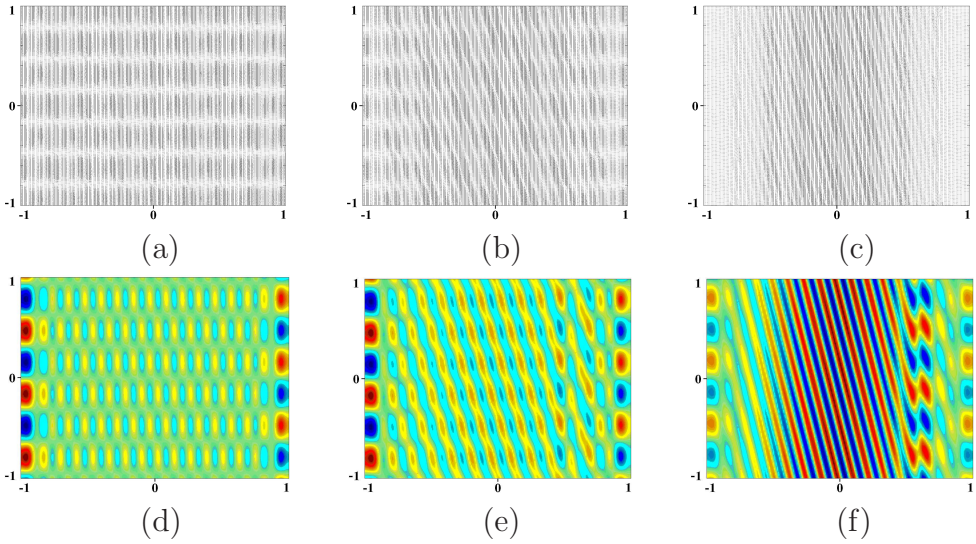

Figure 7: Distributions of the perturbations of the velocity (a – c) and temperature (d – f) of *Flow 1* with $g = g_0 \cdot 10^{-4}$, $\varepsilon = 0.01$, $\alpha = 10$, $\lambda = 0.4$: a), d) — Pe = 0.002; b), e) — Pe = 0.02; c), f) — Pe = 0.2.

With the growing Reynolds number a reverse transition from the rhombic cells (under small Re_m, Fig. 13, c) to the polygonal structures elongated lengthwise the flow axis (with large Re_m occurs, Fig. 13, a). The typical fields of the temperature perturbations are completely identical to those observed with the changing linear size.

Thus, for the spatial perturbations the problem under consideration has a full spectrum. It leads to the existence of a wider family of possible convective regimes in comparison with the plane case. For the non-isothermal flows the temperature disturbances can have the form of the thermal rolls, thermal "spots" or hydrothermal shafts. The family of the characteristic perturbations of the temperature for the isothermal *Flow 2* is not as rich, than for the non-isothermal *Flow 1* and *Flow 3*; and even more, the convective structures of the hydrothermal shaft type are not formed, since the energy transfer from the basic flow to the perturbation does not occur. The velocity perturbations of *Flow 2* can induce the appearance of the polygonal patterns having a certain symmetry (rhombic and triangular cells), and cells stretched along the flow axis. For all classes of flows the most diversified family of the characteristic perturbations is observed in the case of the short length waves.

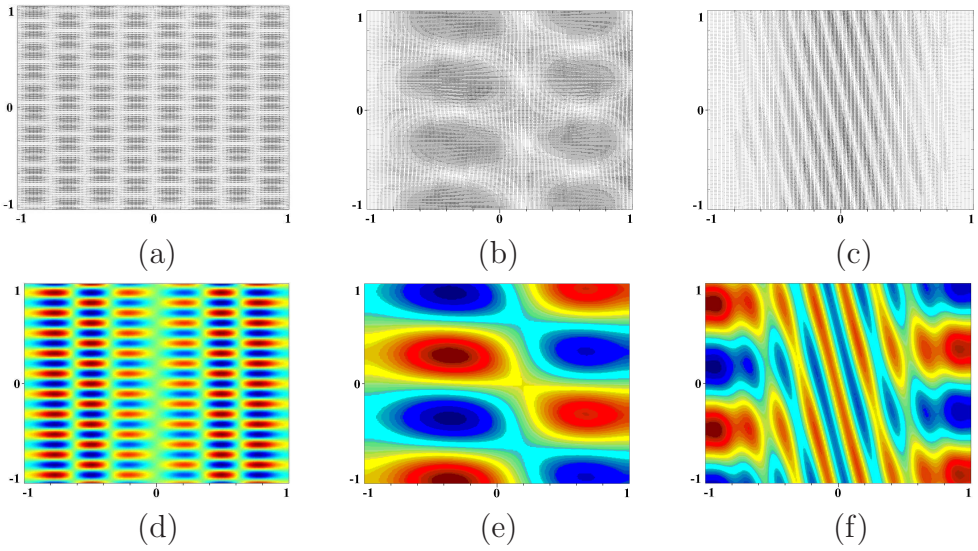

Figure 8: Distributions of the perturbations of the velocity (a – c) and temperature (d – f) of *Flow 1* with $g = g_0 \cdot 10^{-4}$, $\varepsilon = 0.01$, $\alpha = 10$, $\lambda = 1$: a), d) — $a = 0.25$ mm; b), e) — $a = 2$ mm; c), f) — $a = 10$ mm.

6. Instability mechanisms

Let us discuss the physical mechanisms leading to instability and to the formation of the oscillatory regimes. For the non-isothermal *Flow 1* and *Flow 3* the appearance of the convective cells is connected with the horizontal stratification of the temperature of the basic state. If the liquid element moves in the horizontal direction due to random small perturbations, then its density differs from the density of the ambient fluid. As a result, density perturbations which are nonuniform both in the horizontal and vertical direction appear. These disturbances induce the velocity perturbations leading to the formation of the vortices due to the motion of the warmer (and then, lighter) and colder (heavier) fluid. The element travels in the vertical direction induced by the buoyancy force and it can lead to instability. With time the temperature equalization occurs. If the density drops, and accordingly, the buoyancy force decreases, then the perturbations fade out. In another case the instability is developed and it results in the transformation of the basic flow. In the isothermal case the appearance of the convective cells is entirely connected with the temperature deviations induced by the perturbations.

The physical mechanism of the formation of the oscillatory regimes for the non-isothermal *Flow 1* and *Flow 3* is associated with the presence of the

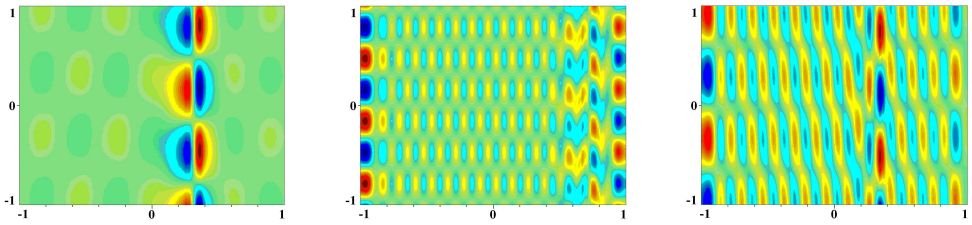

(a) (b) (c)

Figure 9: Distributions of the perturbations of the velocity (a – c) and temperature (d – f) of *Flow 3* with Pe = 0.002, $\alpha = 10$, $\varepsilon = 0.01$: a) — $g = g_0 \cdot 10^{-4}$, $\lambda = 0$; b) — $g = g_0 \cdot 10^{-4}$, $\lambda = 0.5$; c) — $g = g_0 \cdot 10^{-2}$, $\lambda = 1$.

transversal velocity and temperature stratification in the horizontal direction. If $\lambda \neq 0$ the perturbations interacting with the basic flow are shifted along the channel both upwards (near the hot wall) and downwards (near the cold wall), and across the channel (due to the non-zero component of the velocity u_0). A small liquid element accidentally traveling in the horizontal direction keeps moving along the axis x due to the transversal velocity u_0, but the arising buoyant power forces the element to move in the vertical direction due to the density drop. Thus, a small liquid volume oscillates in the vertical and horizontal direction. The corresponding mode is essentially connected with the non-isothermality of the basic flow.

In the common case, the spectral problems with respect to the Grashof number Gr under $\lambda \neq 0$, Peclet number Pe with $\lambda = 0$ (for the "spiral" perturbations) for the non-isothermal *Flow 1* and *Flow 3*, respectively, and Reynolds number Re for the isothermal *Flow 2* were solved to define the stability boundaries and variations in the critical characteristics with the basic parameters.

The dependence of the critical parameters of instability are presented in Fig. 14, $16 - 18$. In all the figures the instability regions are above the curves/surfaces; the numbers of the curves $1 - 3$ and subscripts of the parameters correspond to the flow types.

The plane perturbations are the most dangerous ones for the non-isothermal flows. In Fig. 14 the dependences of the critical Grashof number on the λ parameter are shown. The curves were constructed under the critical wave numbers $\alpha_{*1} = 1.14$, $\alpha_{*3} = 0.86$ for *Flow 1* and *Flow 3* respectively. The minimal critical values $\mathrm{Gr}_{*1} = 431.12$, $\mathrm{Gr}_{*3} = 307.91$ of the monotonic instability are reached with these values of α_*. The points $A(\varepsilon, \mathrm{Gr}_*)$ in Fig. 14, b

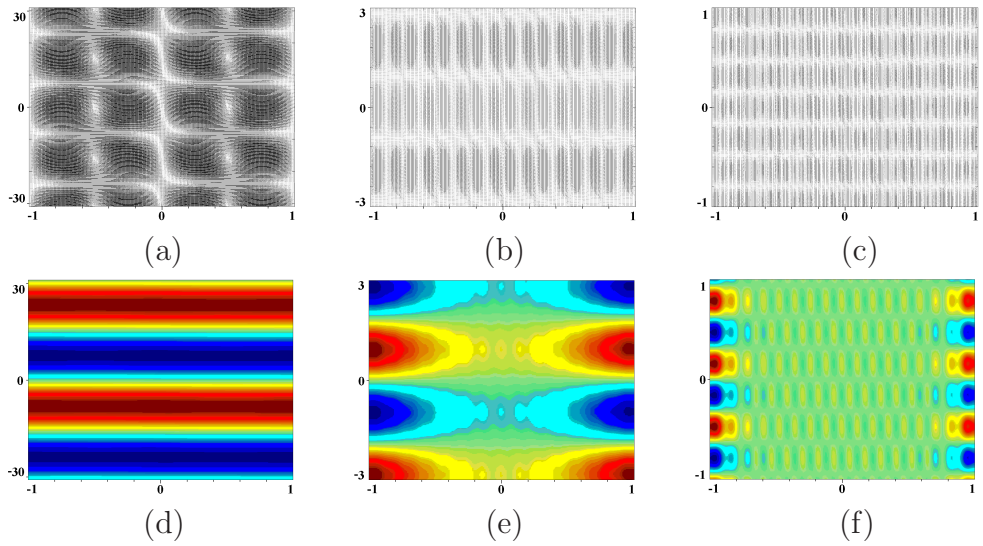

Figure 10: Distributions of the perturbations of the velocity (a – c) and temperature (d – f) of *Flow 2* with $g = g_0 \cdot 10^{-4}$, $\mathrm{Re}_m = 0.655$, $\varepsilon = 0.01$, $\lambda = 1$: a), d) — $\alpha = 0.2$; b), e) — $\alpha = 5$; c), f) — $\alpha = 10$.

specify the parameter values at which the change of the the most dangerous critical mode is observed. On the left hand of the points A the region of the monotonic instability is located, on the right hand of the points A the domain of the oscillatory instability is situated.

The points have the coordinates $A_1(0.067, 609.2)$ and $A_3(0.051, 479.4)$ for *Flow 1* and *Flow 3*, respectively. The analysis of the spectrum of the eigenvalues shows that the oscillatory instability is caused by the lower hydrodynamic modes (Fig. 15). The corresponding branches make a pair of the oscillatory perturbations with the common imaginary part beginning from some value of the Grashof number. Therefore, the oscillatory instability is generated by the growing hydrodynamic perturbations in the flux.

In Fig. 16 the highlighted curves on the parametric surface $\mathrm{Gr}(\varepsilon, \mathrm{Pe})$ correspond to the values at which the most dangerous mode changes from monotonic to the oscillatory one. With the further growth of the Peclet number Pe marked stabilization is observed. The critical numbers Gr_* increase without any limit with $\mathrm{Pe} > 0.007$. The transversal flux stabilizes the flow with respect to the hydrodynamic modes, with the growing Peclet number the lower levels of the spectrum decrease.

For *Flow 1* and *Flow 3* the instability regions with regard to the "spiral"

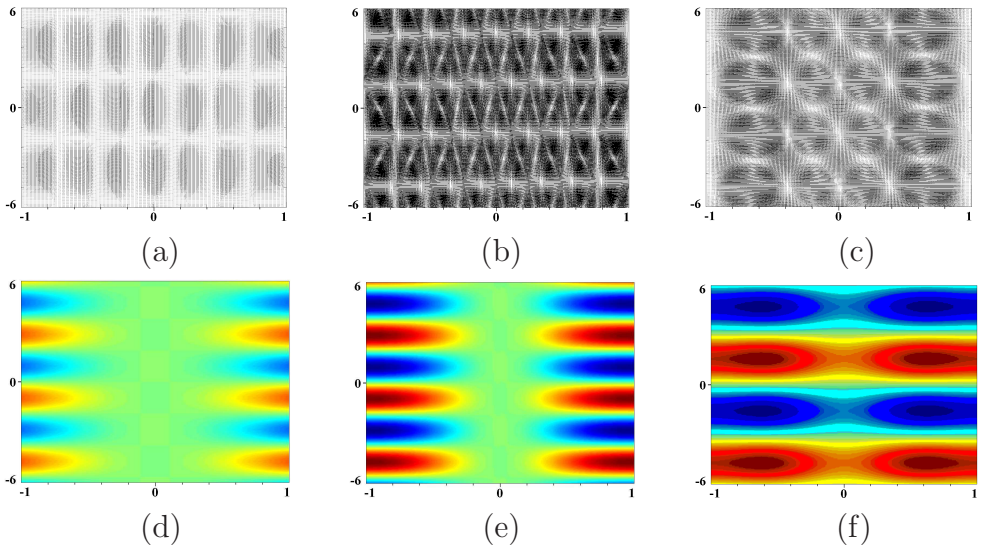

Figure 11: Distributions of the perturbations of the velocity (a – c) and temperature (d – f) of *Flow 2* with $g = g_0 \cdot 10^{-4}$, $\mathrm{Re}_m = 0.655$, $\varepsilon = 0.01$, $\alpha = 1$: a), d) — $\lambda = 0$; b), e) — $\lambda = 0.2$; c), f) — $\lambda = 0.6$.

perturbations were not found in the calculated ranges of the parameters values $0.001 \leq \alpha \leq 10$ and $10^{-3} \leq \varepsilon \leq 0.1$. The stability with respect to the shortwave "spiral" perturbations were analytically proved in [33].

For the isothermal *Flow 2* the critical characteristic is Re_m^*, and the dependences $\mathrm{Re}_m^*(\alpha, \lambda)$ and $\mathrm{Re}_m^*(\mathrm{Gr})$ are shown in Fig. 17.

The critical wave numbers α_* are slightly changed in the considered domain of the values of the problem parameters. With $\mathrm{Gr} = 185$, $\lambda = 1$ the threshold $\mathrm{Re}_{m1}^* = 1.12$ is reached with $\alpha_{*1} = 2.2$. If $\lambda = 0.5$, then the threshold is $\mathrm{Re}_{m2}^* = 2.28$ with $\alpha_{*2} = 2.34$ (Fig. 17, a).

Since the critical Reynolds number almost does not depend on the Boussinesq parameter ε, then the character of the dependence $\mathrm{Re}(\mathrm{Gr})$ suggests that geometrical sizes of the system and gravity influence the threshold. The growing thickness of the layer and/or gravity stabilize the flow (Fig. 17, b). Furthermore, the change of the critical mode was not observed for this class of flows.

In the general case for the oscillatory disturbances of the microconvective non-isothermal flows the type of instability depends on the wave length of the perturbations and also on the viscous and thermal properties of the medium (Fig. 18). With the small Prandtl numbers the hydrodynamic mechanism is

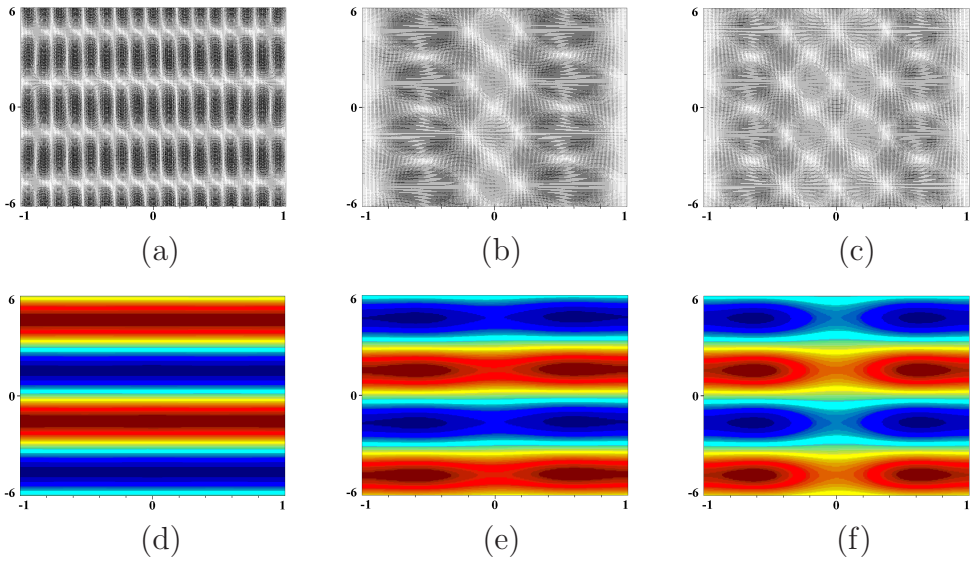

Figure 12: Distributions of the perturbations of the velocity (a – c) and temperature (d – f) of *Flow 2* with $\mathrm{Re}_m = 0.655$, $\varepsilon = 0.01$, $\alpha = 1$, $\lambda = 0.8$: a), d) — $g = g_0 \cdot 10^{-6}$; b), e) — $g = g_0 \cdot 10^{-4}$; c), f) — $g = g_0 \cdot 10^{-2}$.

the basic mechanism of instability.

If Pr is higher than the critical value Pr_*, then the change of the instability regimes is possible. With $\alpha < \alpha_*$ the hydrodynamic mode is the most dangerous one. Upon this, the instability is induced by the growing hydrodynamic perturbations at the boundary of the opposite currents. With $\alpha \geq \alpha_*$ the transition to the thermal mode occurs and the instability is originated by the non-isothermality of the main flow, since for *Flow 2* a similar change of the dangerous modes was not found.

The critical values $(\mathrm{Pr}_*, \alpha_*)$ for *Flow 1* and *Flow 3* are (9.84, 1.28) and (8.47, 2.41), respectively. The oscillatory instability with the large Prandtl numbers is originated by the growing temperature disturbances in the form of the traveling thermal waves. The thermal mechanism of the instability associated with the generation of thermal waves in fluids with the high Prandtl number is also found in the stability problems solved in the framework of the Oberbeck – Boussinesq model [39].

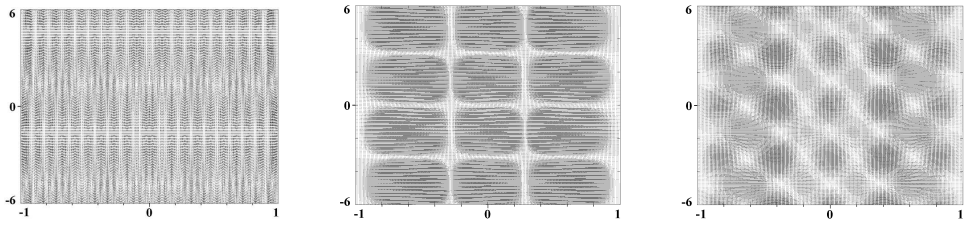

Figure 13: Distributions of the perturbations of the velocity (a – c) and temperature (d – f) of *Flow 2* with $g = g_0 \cdot 10^{-4}$, $\varepsilon = 0.01$, $\alpha = 1$, $\lambda = 1$: a) — $a = 0.25$ mm; b) — $a = 2$ mm; c) — $a = 10$ mm.

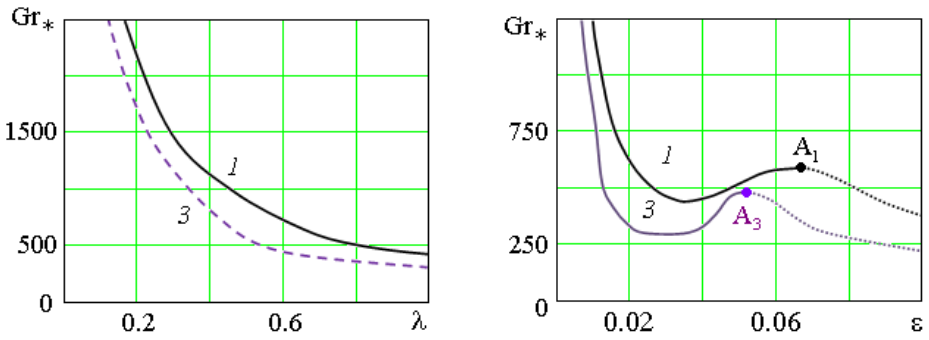

Figure 14: Dependence of the critical Grashof number on the problem parameters with $\mathrm{Pe} = 0.002$: a) — $\varepsilon = 0.037$; b) — $\lambda = 1$.

7. Conclusions

The exact invariant solution describing the fluid flow in the vertical channel under the non-Boussinesq condition was investigated. The classification of the flow types was suggested, depending on the values of the problem parameters and boundary conditions for the temperature function.

The properties of the spatial nonstationary characteristic perturbations of all the classes of flows in the vertical channel with the given temperature on the channel walls were studied. The typical patterns of the disturbances were presented.

The temperature perturbations can lead to the formation of thermal rolls or thermal spots. The velocity disturbances form celullar or polygonal structures, and among them, those with the complex spatial configuration and their sizes depend on the wavelength of the perturbation. Furthermore, the

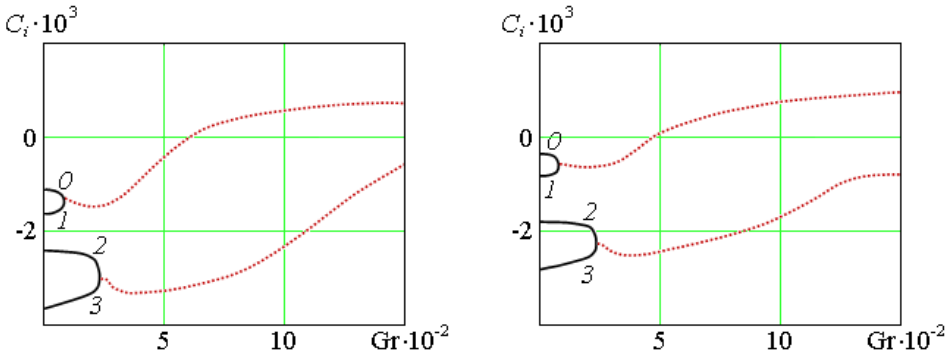

Figure 15: Decrements of the lower hydrodynamic levels with $\varepsilon = 0.07$, $\lambda = 1$, *0–3* are the level of the spectrum: a) — *Flow 1*; b) — *Flow 3*.

formation of hydrothermal oblique shafts is possible. The influence of the thermal load on the channel boundaries, transversal size of the channel and gravity on the type of the characteristic perturbations and structure of the spectrum was investigated. The dependences of the perturbation decrements on the wave number and critical characteristics of the stability were obtained in the space of the problem parameters. On the basis of the calculations series the oscillatory character of the perturbations were defined. It is explained by the non-self-adjacency of the operator of the corresponding spectral problem.

Acknowledgements. This work was partially supported by the Government of the Russian Federation, grant for studying under the supervision of leading scientists in the Siberian Federal University (project 14.Y26.31.0006).

References

[1] V.S. Avduevskii, V.I. Polezhaev (eds.), Hydrodynamics, Heat and Mass Transfer in Weightlessness, Nauka, Moscow, 1982. [in Russian]

[2] H.U. Walter (ed.), Fluid Science and Material Science in Space, Springer-Verlag, Berlin, 1987.

[3] V.I. Polezhaev, Convection and Heat/Mass Transfer Processes under Space Flight Conditions, Fluid Dyn. 41(5) (2006) 736-754.

[4] C.B. Sobhan, G.P. Peterson, Microscale and Nanoscale Heat Transfer:

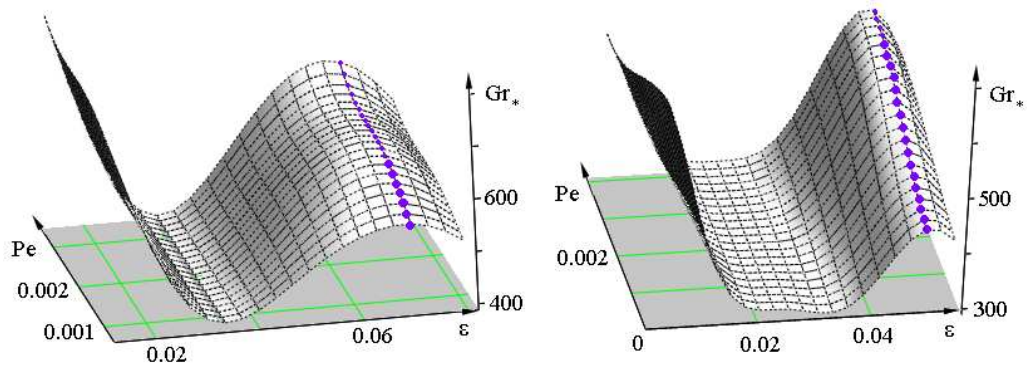

(a) (b)

Figure 16: Dependence of the critical Grashof number on the Boussinesq parameter ε and Peclet number Pe with $\lambda = 1$: a) — *Flow 1*, $\alpha = 1.14$; b) — *Flow 3*, $\alpha = 0.86$.

Fundamentals and Engineering Applications, CRC Press Taylor and Francis Group, 2008.

[5] M. Rebay M, S. Kakaç, R.M. Cotta, Microscale and Nanoscale Heat Transfer: Analysis, Design, and Application, CRC Press Taylor and Francis Group, 2016.

[6] G. Müller, Convection and Inhomogeneities in Crystal Growth from the Melt, Springer-Verlag, Berlin, 1988.

[7] I.L. Shul'pina, B.G. Zakharov, R.V. Parfen'ev, I.I. Farbshtein, Yu.A. Serebryakov, I.A. Prokhorov, Some results of the growth of semiconductor crystals in microgravity conditions (to the 50th anniversary of Yuri Gagarin's flight into space), Physics of the Solid State 54(7) (2012) 1340-1344.

[8] V.I. Strelov, I.P. Kuranova, B.G. Zakharov, A.E. Voloshin, Crystallization in space: Results and prospects, Crystallography Reports 59(6) (2014) 781-806.

[9] A.P. Lebedev, V.I. Polezhaev, The mechanics of weightlessness: microaccelerations and gravitational sensitivity of mass transfer processes associated with the manufacture of materials in space, Uspekhi Mechaniki 13(1) (1990) 3-51. [in Russian]

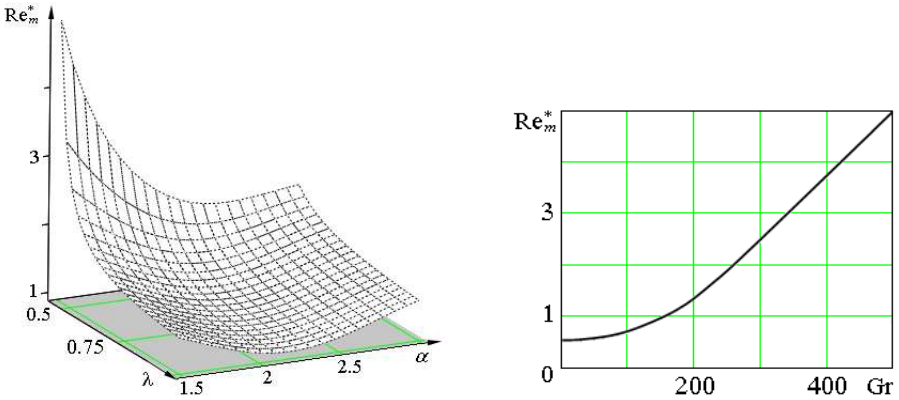

(a) (b)

Figure 17: Dependence of the critical Reynolds number Re_m^* on the problem parameters: a) — $\varepsilon = 0.037$, $\mathrm{Gr} = 185$; b) — $\varepsilon = 0.037$, $\lambda = 1$, $\alpha = 2.2$.

[10] O.A. Bessonov, V.A. Brailovskaya, V.I. Polezhaev, Three-dimensional effects of convection in alloys: Concentration nonuniformities, onset of asymmetry and oscillations, Fluid Dyn. 32(3) (1997) 379-386.

[11] F. Otalora, J.M. Garcia-Ruiz, Crystal growth studies in microgravity with the APCF. I. Computer simulation of transport dynamics, J. of Crystal Growth 182(1-2) (1997) 141-154.

[12] J.M. Garcia-Ruiz, F. Otalora, Crystal growth studies in microgravity with the APCF. II. Image analysis studies, J. of Crystal Growth 182(1-2) (1997) 155-167.

[13] T. Maekawa, Y. Hiraokaa, K. Ikegamia, S. Matsumotob, Numerical modeling and analysis of binary compound semiconductor growth under Microgravity conditions, J. of Crystal Growth 229(1-4) (2001) 605-609.

[14] N.V. Nikitin, S.A. Nikitin, V.I. Polezhaev, Convective instabilities in a Czochralski hydrodynamic model, Uspekhi mechaniki 2(4) (2003) 63-105. [in Russian]

[15] V.V. Pukhnachov, Mathematical model of natural convection under low gravity, IMA Preprint Series, University of Minnesota, Minneapolis, 1991.

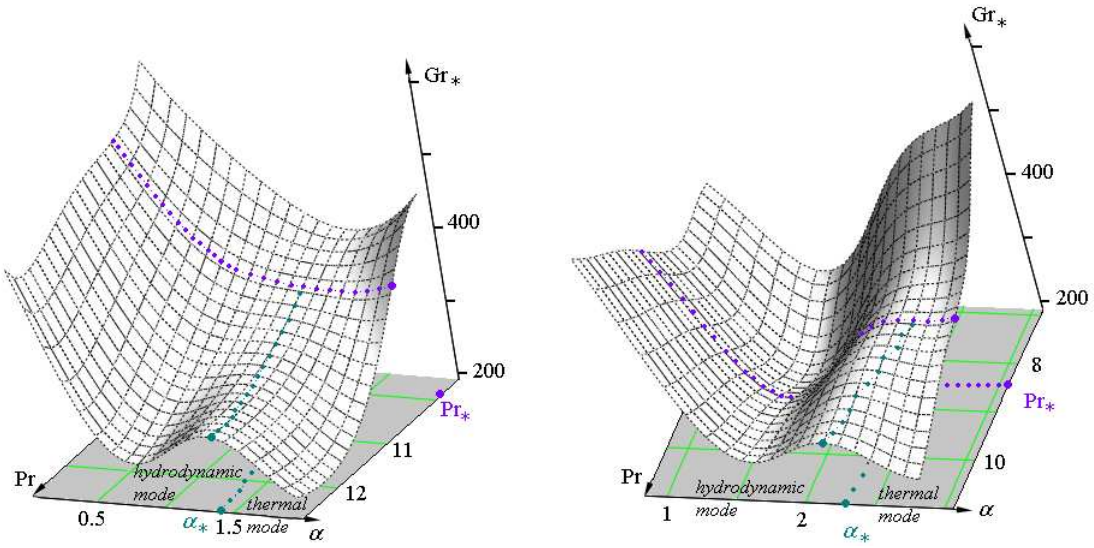

Figure 18: Dependence of the critical Grashof number on the Prandtl number Pr and wave number α with $\varepsilon = 0.03$, Pe $= 0.002$, $\lambda = 1$: a) — *Flow 1*; b) — *Flow 3*.

[16] V.V. Pukhnachov, Model of convective motion under low gravity, In Proceedings VIIIth European Symposium on Materials and Fluid Sciences in Microgravity, Brussels (Belgium), 12/16 April 1992, ESA SP, 157-160.

[17] V.V. Puknachev, Model of convective motion under low gravity, Model. Mekh. 6(4) (1992) 47-56. [in Russian]

[18] P.S. Perera, R.F. Sekerka, Nonsolenoidal flow in a liquid diffusion couple, Phys. Fluids 9(2) (1997) 376-391.

[19] V.I. Polezhaev, A.V. Bune, N.A. Verezub, G.S. Glushko, V.L. Gryaznov, K.G. Dubovik, et al., Mathematical modeling of convective heat and mass exchange on basis of the Navier – Stokes equations, Nauka, Moscow, 1987. [in Russian]

[20] V.K. Andreev, O.V. Kaptsov, V.V. Pukhnachev, A.A. Rodionov, Applications of Group-Theoretical Methods in Hydrodynamics, Springer, Netherlands, 1998.

[21] V.I. Polezhaev, M.S. Bello, N.A. Verezub, K.G. Dubovik, A.P. Lebedev, S.A. Nikitin, et al., Convective Processes in Weughtlessness, Nauka, Moscow, 1991. [in Russian]

[22] V.K. Andreev, Yu.A. Gaponenko, O.N. Goncharova, V.V. Pukhnachev, Mathematical Models of Convection, Walter de Gruyter, Berlin/Boston, 2012.

[23] R. Monti (ed.), Physics of Fluids in Microgravity, 1st ed, Routledge, Florence, 2002.

[24] V.I. Polezhaev, A.A. Gorbunov, E.B. Soboleva, Unsteady near-critical flows in microgravity environment, Transport Phenomena in Microgravity. Ann. N.Y. Acad. Sci. 1027 (2004) 286-302.

[25] A.A. Rodionov, Group analysis of microconvection equations and one nonclassical equation, Proc. Workshop Mathematical Modeling in Mechanics, Inst. Comp. Math., Sib. Branch, Russian Acad. of Sci., Krasnoyarsk (1999), 169-180. (Deposited at VINITI 05.07.1999, No. 1999-B99). [in Russian]

[26] V.V. Pukhnachov, Microconvection in a vertical layer, Fluid Dynamics, 29(5) (1994), 653-660.

[27] A.A. Rodionov, Some exact solutions of microconvection equations, In Symmetry and Differential Equations, Krasnoyarsk (2000), 186-189. [in Russian]

[28] V.B. Bekezhanova, Stationary solution of the equations of microconvection in a vertical layer, J. Appl. Mech. Techn. Phys. 42(3) (2001) 437-444.

[29] O.N. Goncharova, Mathematical models of convection under microgravity conditions, Doctor's dissertation, Novosibirsk, 2005. [in Russian]

[30] Yu. A. Gaponenko, V.E. Zakhvataev, Nonboussinesq Thermal Convection in Microgravity under Nonuniform Heating, J. Appl. Mech. Techn. Phys. 43(6) (2002) 823-829.

[31] O.N. Goncharova, Microconvection in weak force fields. A numerical comparison of two models, J. Appl. Mech. Techn. Phys. 38(2) (1997) 219-223.

[32] V.B. Bekezhanova, Stability of steady nonisothermal flow in a vertical layer with permeable boundaries in the microconvection model, Fluid Dyn. 41(3) (2006) 343-350.

[33] V.B. Bekezhanova, I.A. Shefer, Microconvection in vertical channel at given heat flux, J. Phys: Conference Ser. 754 (2016) 022001.

[34] V.K. Andreev, V.B. Bekezhanova, Stability of the equilibrium of a flat layer in a microconvection model, J. Appl. Mech. Techn. Phys. 43(2) (2002) 208-216.

[35] V.K. Andreev, E.A. Ryabitskii, Origination of Microconvection in a Flat Layer with a Free Boundary, J. Appl. Mech. Techn. Phys. 45(1) (2004) 22-30.

[36] V.K. Andreev, V.B. Bekezhanova, Stability of Nonisothermal Fluids, Siberian Federal University, Krasnoyarsk, 2010. [in Russian]

[37] V.V. Pukhnachov, Solvability of initial boundary value problem in non-standard model of convection. J. Math. Sci. 93 (1999) 772-778.

[38] V.V. Pukhnachov, Stationary problem of the microconvection, In Collection of research papers of the Siberian Branch of the Russian Academy of Sciences "Dynamics of continuous medium", Institute of Hydrodynamics, 111 (1996) 109-116.

[39] G.Z. Gershuni, E.M. Zhukhovitskii, Convective Stability of an Incompressible Fluid, Nauka, Moscow, 1972. [in Russian]

[40] E. Kamke, Differentialgleichungen, I. Gewöhnliche Differentialgleichungen, Springer, New York, 1997.

[41] A.S. Monin, Hydrodynamic instability, Sov. Phys. Usp. 29(9) (1986) 843-868.

[42] S.K. Godunov, On the numerical solution of boundary-value problems for systems of linear ordinary differential equations, Uspekhi Mat. Nauk, 16 (1961) 171-174. [in Russian]

[43] A.A. Abramov, On the transfer of boundary conditions for systems of ordinary linear differential equations (a variant of the dispersive method), USSR Computational Math. and Math. Phys. 1 (1962) 617-622.